Natural gas sweetening using tailored ionic liquid-methanol mixed solvent with selective removal of H_2S and CO_2

Lei, Yang; Du, Lei; Liu, Xinyan; Yu, Haoshui; Liang, Xiaodong; Kontogeorgis, Georgios M.; Chen, Yuqiu

Published in:
Chemical engineering journal

DOI (link to publication from Publisher):
10.1016/j.cej.2023.146424

Publication date:
2023

Document Version
Publisher's PDF, also known as Version of record

Chemical Engineering Journal 476 (2023) 146424

Contents lists available at ScienceDirect

Chemical Engineering Journal

journal homepage: www.elsevier.com/locate/cej

Natural gas sweetening using tailored ionic liquid-methanol mixed solvent with selective removal of H_2S and CO_2

Yang Lei [a], Lei Du [a], Xinyan Liu [a], Haoshui Yu [b,*], Xiaodong Liang [c], Georgios M. Kontogeorgis [c], Yuqiu Chen [c,*]

[a] School of Chemistry and Chemical Engineering, Hubei Key Laboratory of Coal Conversion and New Carbon Materials, Wuhan University of Science and Technology, Wuhan 430081, Hubei, China
[b] Department of Chemistry and Bioscience, Aalborg University, Niels Bohrs Vej 8A, Esbjerg 6700, Denmark
[c] Department of Chemical and Biochemical Engineering, Technical University of Denmark, DK-2800 Lyngby, Denmark

ARTICLE INFO

Keywords:
Natural gas
H_2S and CO_2 removal
Ionic liquids
Mixed solvent
Process design

ABSTRACT

Natural gas is often preferred in various energy applications due to its many advantages over conventional fossil fuels such as oil and coal. However, the removal of pollutants from natural gas, particularly hydrogen sulfide (H_2S) and carbon dioxide (CO_2), requires complex treatment strategies, significantly impacting the cost of natural gas production. In this work, we propose a mixed solvent combining ionic liquid (IL) and methanol, which can selectively and simultaneously remove H_2S and CO_2 by customizing the IL structure and its ratio in the solvent. This purification process offers improved efficiency and energy savings compared to traditional methods. To determine the optimal IL structure in the mixed solvent, a computer-aided design method was employed. Through solving the formulated MINLP problem, the IL 1-methyl pyridinium trifluoroacetate ([C_1OHPy][TFA]) was identified as having the highest affinity for H_2S, making it suitable for use in the IL-methanol mixed solvent. Furthermore, the upgrading process of high-sulfur natural gas using the IL-methanol mixed solvent was simulated and evaluated, comparing it to the benchmark natural gas upgrading (Rectisol) process. The results demonstrate that the IL-methanol mixed solvent natural gas upgrading process achieved a 55.57 % power savings and reduced the annual total cost (TAC) by 23.90 % compared to the Rectisol process. These findings highlight the significant potential of our tailored IL-methanol mixed solvent in natural gas production.

1. Introduction

Natural gas, mostly identified as a clean energy source, has become one of the most attractive fossil fuels in the world's supply of energy [1,2]. Besides its primary use as a fuel, natural gas is also an important source of hydrocarbons for petrochemical feedstocks. Nature gas has diverse energy-related applications from industrial use to the production of electricity. In contrast to conventional fossil fuels such as gasoline and diesel, natural gas produces much less CO_2, SO_2, and NO_x, with no particulate matter emissions, and thereby has reduced adverse impaction on the climate and the environment. The increase in natural gas supply provides a prospect for meeting the world's growing demand for clean energy in the future. However, raw natural gas usually contains many impurities (*e.g.* CO_2, H_2S, C_{2+}), and the presence of these impurities is often associated with severe corrosion problems that can damage the equipment system and even lead to pipe rupture [3]. H_2S with the characteristic foul odor of rotten eggs is very poisonous, corrosive, and flammable [4]. It must be noted that H_2S presents odorless when its concentration in the air exceeds a certain value. CO_2 is another major acid gas contaminant and its presence contributes to a major cause of the corrosion problems. Therefore, these impurities especially H_2S and CO_2 need to be removed from natural gas to meet the criteria of the pipeline transportation and the quality standards of the gas products [5–7]. The removal of such impurities remains one of the most critical concerns in the natural gas industry [8].

To date, various separation methods for gas upgrading have been investigated, each with its advantages and limitations. Among them, the absorption process is a major commercial technology, that has been widely used in industry to treat natural gas. Generally, chemical solvents such as 6-Ethyl-o-toluidine (MEA), diethanolamine (DEA), triethanolamine (DEA), diisopropylamine (DIPA), or methyl diethanolamine (MDEA) have higher absorption capacity but have higher energy

* Corresponding authors.
E-mail addresses: hayu@bio.aau.dk (H. Yu), yuqch@kt.dtu.dk (Y. Chen).

https://doi.org/10.1016/j.cej.2023.146424
Received 20 June 2023; Received in revised form 14 September 2023; Accepted 2 October 2023
Available online 5 October 2023

Table 1
Reported ILs for removal of H_2S and CO_2.

	Full name	Abbreviations	Remark	Refs.
Desulfurization and decarbonization	1-ethyl-3-methylimidazolium bis(trifluoromethyl sulfonyl)-imide	[EMIM][Tf_2N]	IL-methanol mixed solvent	[44]
	1-ethyl-3-methylimidazolium bis dihydrogen phosphate	[EMIM][H_2PO_4]		[4]
	1-butyl-3-methylimidazolium bis(trifluoromethylsulfonyl)-imide	[BMIM][NTf_2]		[37]
	3-methyl-1-ethylpyridinium bis(tri-fluoromethylsulfonyl)-imide	[3MEPYNT F_2]		[45]
	quaternary ammonium polyether	TEGO ILK5		[46]
	Nbutylpyridinium thiocyanate	[C_4Py][SCN]		[47]
	1-ethyl-3-methylimidazolium ethylsulfate	[EMIM][$EtSO_4$]		[31]
	1-(2-hydroxyethyl)-3-methylimidazolium tetrafluoroborate	[HEMIM][BF_4]		[48]
	1-octyl-3-methylimidazolium hexafluorophosphate	[C_8MIM][PF_6]		[49]
	1-butyl-3-methylimidazolium methylsulfate	[BMIM][$MeSO_4$]		[50,51]
	Tri-hexyltetradecylphosphonium Bis(trifluoromethylsulfonyl)-imide	[P_{6614}][NTf_2]		[30]
	1-butyl-3-methylimidazolium bis(trifluoromethylsulfonyl)-imide	[C_4MIM][NTf_2]		[30]
	1-butyl-3-methylimidazolium methanesulfonate	[C_4MIM][CH_3SO_3]		[52]
	1-ethyl-3-methylimidazolium tris(pentafluoroethyl) trifluorophosphate	[EMIM][FAP]		[53]
	1-butyl-3-methylimidazolium bromide	[BMIM][Br]		[2]
Decarburization	*N*-methyl-2-hydroxyethylammonium propionate	2mHEAPr		[52]
	l-ally1-3-methylimidazolium bis(trifluoromethyl sulfonyl)-imide	[AMIM][Tf_2N]	IL-methanol mixed solvent	[43]
	triethyl(octyl)phosphonium 2-cyanopyrrole	[P228][CNPyr]		[54]
	1-Ethyl-3-methylimidazolium Hydrogensulfate	[EMIM][HSO_4]		[30]
	1-Ethy1-3-methylimidazolium Methylsulfate	[EMIM][$MeSO_4$]		[30]
	1-Ethyl-3-methylimidazolium Methanesulfonate	[EMIM][$MeSO_3$]		[30]
	1-Ethyl-3-methylimidazoliumThiocyanate	[EMIM][SCN]		[30]
	Ethyl(tributyl)phosphonium Diethylphosphate	[P_{2444}][DEP]		[30]
	1-Hexyl-3-methylimidazoliumTrifluoromethanesulfonate	[HMIM][OTF]		[30]
	1-(2-hydroxyethyl)-3-methylimidazolium Trifluoroacetate	[OH EMIM][TFA]		[30]
	1-butyl-3-methylimidazolium trifluoromethanesulfonate	[BMIM][OTF]		[54]
	1-Octyl-3-methylimidazolium Bis(trifluoromethylsulfonyl)imide	[OMIM][Tf_2N]	IL-methanol mixed solvent	[55]
Desulfurization	1-butyl-3-methylimidazolium tetrafluoroborate	[BMIM][BF_4]		[56]
	1-butyl-3-methylimidazolium bis(trifluoromethylsulfonyl)-imide	[BMIM][PF_6]		[56]
	1-Ethyl-3-methylimidazolium hexafuorophosphate	[EMIM][PF_6]		[57]
	1-Ethyl-3-methylimidazolium tris(pentafuoroethyl) trifuorophosphate	[EMIM][EFAP]		[57]
	1-Hexyl-3-methylimidazolium bis(trifuoromethanesulfonyl)imide	[HMIM][Tf_2N]		[57]
	1-Hexyl-3-methylilmidazolium hexafuorophosphate	[HMIM][PF_6]		[57]
	1-*n*-Octyl-3-methylimidazolium hexafuorophosphate	[OMIM][PF_6]		[57]
	1-(2-Hydroxyethyl)-3-methylimidazolium bis(trifuoromethylsulfonyl) imide	[HOeMIM][Tf_2N]		[57]
	1-(2-Hydroxyethyl)-3-methylimidazolium trifuoromethanesulfonate	[HOeMIM][OTF]		[57]
	1-(2-Hydroxyethyl)-3-methylimidazolium hexafuorophosphate	[HOEMIM][PF_6]		[57]

requirements for solvent regeneration. For feed gas with low temperature and high acid gas concentration, the physical solvent method is preferred [5,9,10]. The Selexol process uses a physical solvent made from polyethylene glycol dimethyl ether (DEPG) and is selective for removing sulfur compounds, but generally does not remove enough carbon dioxide to meet pipeline gas requirements [11]. Glyceryl carbonate is another physical solvent with high selectivity for CO_2 removal, but its ability is relatively low. In most cases, chemical and physical solvents (such as MEA [12], MDEA, and DEPG) are selective for removing H_2S or CO_2, making it difficult to meet pipeline specifications for both H_2S and CO_2 [10,13]. In addition, in the process of natural gas purification using these organic solvents, solvent loss is also encountered due to its high volatility and high energy required for regeneration. In industrial operations, qualified natural gas can be obtained at the cost of using large quantities of solvents. However, such gas treatment schemes will significantly increase equipment size and energy consumption [14]. In addition, the membrane separation method is also commonly used in the process of removing acidic gases. Membrane separation can quickly and effectively remove hydrogen sulfide and carbon dioxide from the mixed gas. Compared with traditional absorbent desulfurization and decarbonization methods, membrane separation has the advantages of lower energy consumption [15], energy saving [16], simple operation [17], and a small equipment footprint [18]. However, in the process of natural gas desulfurization and decarbonization, membrane separation also has some drawbacks. Besides hydrogen sulfide and carbon dioxide, natural gas may also contain other impurities, which could affect the effectiveness of membrane separation, leading to poor desulfurization and decarbonization effects. Additionally, after long-term operation, the membrane separation device may become contaminated and damaged by impurities, requiring regular cleaning and maintenance. The initial investment in membrane separation equipment is relatively high, and economic cost considerations need to be taken into account. Furthermore, membrane separation requires high gas pressure and purity. If natural gas contains high concentrations of hydrogen sulfide and carbon dioxide, pretreatment is necessary to make it suitable for membrane separation. Therefore, an absorbent capable of controlling the removal of both H_2S and CO_2 is much needed, as it can provide a universal alternative for the treatment of natural gas with different concentrations of H_2S and CO_2.

In addition, Rectisol is a mature and effective method to remove acid gas through physical absorption [19–21]. The process uses cooling methanol as solvent and deep removal of sulfur-containing compounds (H_2S, COS) and CO_2 in the treatment gas. Compared with other physical solvents, methanol is more selective to acid components and requires less solvent. The methanol solvent process using methanol as a solvent has been widely used in industry due to its advantages over other physical solvents (such as non-corrosion, low viscosity, and availability). However, due to the high vapor pressure of methanol, the cryogenic methanol washing process must be operated at very low temperatures, which may result in large solvent losses and large power consumption

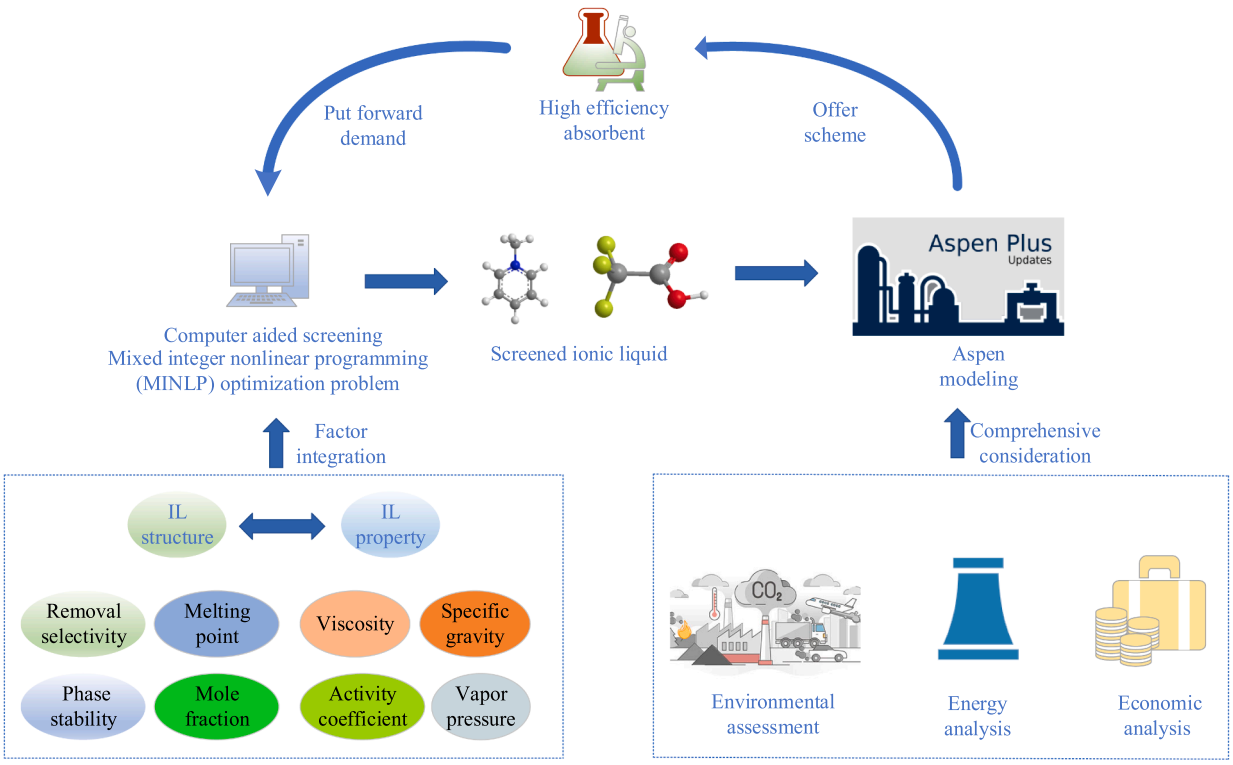

Fig. 1. Modeling strategy for natural gas desulfurization and decarbonization.

[22–24].

Ionic liquids (ILs) are considered potential substitutes for organic solvents in many chemical and biochemical processes due to their attractive solvent properties such as non-volatility, low melting point [25], high thermal stability [26,27], and chemical stability [28–33]. So far, ILs have been extensively studied as a solvent for separation processes, including gas separation processes such as CO_2 capture [34–36], shale gas purification [37–41], and gaseous isoprene recovery [42–44]. However, these gas separation processes are often limited to the high viscosity and high cost of ILs. On the other hand, the use of methanol with low viscosity and high availability is usually limited by its high vapor pressure. It is conceivable that a mixed solvent combining IL and methanol, with the advantages of both IL and methanol, could provide a potential alternative in the gas separation process [41,42].

There have been many attempts to use ILs for the gas removal of CO_2 and H_2S. The ILs reported for absorbing H_2S and CO_2 are listed in Table 1. However, so far, there are few studies on the use of IL-methanol mixed solvent in the separation process, and no studies on its simultaneous removal of H_2S and CO_2 have been reported. Mohsen et al. [43] found in the simulation of CO_2 capture by methanol, IL and their binary mixture that adding IL to methanol can capture CO_2 at a higher temperature. A mature Rectisol process has been widely applied to remove H_2S and CO_2 from natural gas throughout the world. This is because methanol exhibits excellent solubility to acidic gases at low temperatures, especially for H_2S. However, as the absorption temperature increases, the solubility of acidic gases in methanol sharply decreases, requiring the traditional low-temperature methanol washing process to operate at extremely low temperatures, resulting in high operating costs. Moreover, the use of refrigerants during this process contributes significantly to carbon emissions. Adding an IL to methanol allows for the capture of H_2S and CO_2 at higher temperatures. This is due to the heat released during the exothermic absorption process by introducing the IL results in a lower decrease in gas solubility when compared to using pure methanol solvent. Therefore, adding an IL to methanol and capturing acid gases at higher temperatures can compensate for the temperature increase. As a result, when the temperature increases, the solubility of these acidic gases in the IL does not decrease as dramatically as it does in methanol. This has been experimentally validated by Mohsen et al. [43]. Although the use of IL-methanol mixed solvents offers unexpected opportunities for the upgrade of natural gas, there are still some challenging issues that need to be addressed before its practical application. Firstly, it is very essential to find a suitable IL due to different ILs generally present with very distinct properties and separation performances, however, the very limited experimental data of the IL-natural gas system is a major challenge in this regard. Secondly, how to effectively control the H_2S/CO_2 selectivity of the mixed solvent corresponding to natural gas with different H_2S and CO_2 concentrations also challenges the upgrading process. Furthermore, the uncertainties in the concentrations of H_2S and CO_2 in natural gas at different times could also be a challenging problem that needs to be dealt with accordingly. Otherwise, deterioration of performance and production losses may occur. Herein this work aims to explore the possibility of using an IL-Methanol mixed solvent for concurrent and selective removal of H_2S and CO_2 by trying to solve the challenging problems described above.

The research motivation of this work is to focus on the problems of complex technology and high energy consumption in the practical application of natural gas desulfurization and decarbonization. To realize energy saving and low-carbon operation of the natural gas decarbonization process, a new modeling strategy for natural gas upgrading based on IL-methanol mixed solvent was proposed for the first time, as shown in Fig. 1. In this process, mixed integer nonlinear programming (MINLP) optimization problems are solved to determine the IL that can meet the separation requirements of natural gas acid gas. The energy, environmental (carbon emissions), and economic performance of the gas upgrading process based on the IL-methanol mixture was comprehensively evaluated using a rigorous simulation model based on Aspen Plus. The application of this IL-methanol design method is demonstrated through a case study for one of the world's largest natural gas purification plants in China.

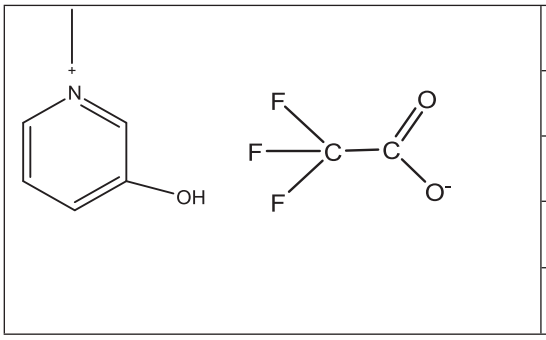

M_{IL} : 224.15 g/mol
T_m : 238.24 K
η : 0.059 $Pa \cdot s$
β_{H_2S,CH_4}: 5270
β_{CO_2,CH_4}: 414

Fig. 2. Structure and some important properties of 1-methyl-3-hydroxyl-pyridinium trifluoroacetate at room temperature.

2. Materials and methods

Currently, experimental data and computational models are the two major approaches used for solvent screening. The experimental-based method is usually preferred since it can provide more reliable results. However, due to a lack of sufficient experimental data on IL-natural gas systems, especially IL-H_2S systems, it is very limited to select suitable ILs to process natural gas containing H_2S. On the other hand, computational models such as physical and thermodynamic property models have been developed or extended to IL and/or IL-gas systems in our previous work [58]. This makes it possible to use a computer-aided design method to find suitable IL-methanol mixed solvents for processing natural gas (see Fig. 2).

It is worth mentioning that the experimental data collected from published works [58,59] were used in the development of the thermodynamic and physical property models. On the other hand, industrial data (composition and flow rate of feedstock, process flow, *etc.*) taken from one of the world's largest natural gas purification plants in China were used for process simulation and to evaluate the reasonableness of the obtained simulation results. The computer-aided solvent design problem is optimized is solved using Python programming. The process simulations are conducted using a well-known commercial process simulator Aspen Plus V11, for which Wuhan University of Science and Technology has the license. The Aspen Economics Analyzer and Aspen Energy Analyzer are utilized for energy and economic analysis, respectively. Furthermore, the net carbon emissions are employed to assess the environmental impact of the processes.

2.1. Formulation of the design problem

In the design problem of IL-methanol mixed solvent, the simultaneous identification of the IL structure and its optimal composition is required. The objective is to maximize the solvent separation performance of the designed IL-methanol solvent, which depends on binary, integer, and continuous variables, while adhering to a series of constraints related to the structural aspects (IL molecule), properties (pure & mixture), and process models (composition). This can be formulated as a mixed-integer non-linear programming (MINLP) optimization problem, described by the following equations:

$max/min_{z,y} f(z,y)$

$s.t. IL structural constraints$:

$$\sum_{i\in C} c_i = 1 \tag{1}$$

$$\sum_{j\in A} a_j = 1 \tag{2}$$

$$\sum_{l=1}^{N} x_l - \sum_{i\in C} c_i v_i = 0 \tag{3}$$

$$\sum_{i\in C}(2 - v_i)c_i + \sum_{l=1}^{N}\sum_{k\in S}(2 - v_{kl})x_l n_{kl} = 2 \tag{4}$$

$$\sum_{k\in S}(2 - v_{kl})x_l n_{kl} = 1 \tag{5}$$

$$n_S^L \le \sum_{l=1}^{N}\sum_{k\in S} x_l n_{kl} \le n_S^U \tag{6}$$

$$n_{Sl}^L \le \sum_{k\in S} x_l n_{kl} \le n_{Sl}^U \tag{7}$$

IL $pure property constraints$:

$$\eta = \exp\left(\sum_{i=1}^{k} n_i a_{i,\eta} + \sum_{i=1}^{k} n_i b_{i,\eta}\frac{100}{T} + \sum_{i=1}^{k} n_i d_{i,\eta}\left(\frac{100}{T}\right)^2\right) * R_{0\eta} < 0.1(Pa \bullet s) \tag{8}$$

$$[52]\ T_m = 288.7 + \sum_{i=1}^{k} n_i \Delta t_i < 298.15(K) \tag{9}$$

IL − methanol $mixture property constraints$:

$$\frac{1}{x_{IL}} + \frac{\partial \ln \gamma_{IL}}{\partial x_{IL}} \ge 0 \tag{10}$$

$$\beta_{H_2S,CH_4} = \frac{P_{CH_4}^S \gamma_{CH_4}^{\infty}}{P_{H_2S}^S \gamma_{H_2S}^{\infty}} > 1000 \tag{11}$$

$$\beta_{CO_2,CH_4} = \frac{P_{CH_4}^S \gamma_{CH_4}^{\infty}}{P_{CO_2}^S \gamma_{CO_2}^{\infty}} > 400 \tag{12}$$

process model constraints :

$$x_{IL} + x_{methanol} = 1 \tag{13}$$

The feasibility and complexity constraints on the IL structure are represented by (Eqs. (1)–(7)), where the sets of cations, anions, and substituents are described as C, A, and S, respectively. The binary variables c_i, α_j, x_l , represent the cations, anions, and side chains l, while the integer variables n_{kl} denote the number of substituents of type k in the side chain l. The vectors of v_C and v_{Sl} represent the group valences of cations and substituents, respectively. Eq. (1) and Eq. (2) indicate that each IL molecule contains only one cation and one anion. The octet rule, expressed in Eq. (3), ensures the consistency between the free valence of the cation and the number of side chains. To prevent more than one covalent bond between any two adjacent groups, (Eqs. (4) and (5)) are

Table 2
Application of IL groups in the design of natural gas desulfurization and decarbonization CAILD.

Types	Groups	Full name	Types	Groups	Full name
Substituents	CH_3	methyl	Cation skeletons	$[IM]^+$	imidazolium
	$CH{=}CH_2$	vinyl		$[MIM]^+$	methyl-imidazolium
	OH	oxhydryl		$[Py]^+$	pyridinium
	CH_2	methylene		$[MPy]^+$	methyl-pyridinium
	CH_3O	methoxy		$[Pyr]^+$	pyrrolidinium
Anions	$[Cl]^-$	chloride		$[MPyr]^+$	methyl-pyrrolidinium
	$[Br]^-$	bromide		$[Pip]^+$	methylpiperidine
	$[BF_4]^-$	tetrafluoroborate		$[MPip]^+$	methylpiperidinium
	$[PF_6]^-$	hexafluorophosphate		$[Morp]^+$	morpholine
	$[TFA]^-$	trifluoroacetate		$[CH_3N]^+$	methanimine
	$[NO_3]^-$	nitrate		$[C_2H_5N]^+$	ethylammonium
	$[TOS]^-$	p-toluenesulfonate		$[C_4H_9N]^+$	buthylammonium
	$[MeSO_4]^-$	methylsulfate		$[C_8H_{17}N]^+$	octylammonium
	$[EtSO_4]^-$	ethylsulfate		$[CH_3P]^+$	methylphosphonium
	$[CH_3SO_3]^-$	methanesulfonate		$[C_2H_5P]^+$	ethylphosphonium
	$[CF_3SO_3]^-$	trifluoromethanesulfonate		$[C_4H_9P]^+$	buthylphosphonium
	$[N(CN)_2]^-$	dicyanamide		$[C_6H_{13}P]^+$	hexylphosphonium
	$[C(CN)_3]^-$	tricyanomethanide		$[C_8H_{17}P]^+$	octylphosphonium
	[B(CN)4]-	tetracyanoborate		$[CH_3S]^+$	methylsulfonium
	$[DMP]^-$	dimethylphosphate		$[C_2H_5S]^+$	ethylsulfonium
	$[Tf_2N]^-$	bis(trifluoromethanesulfonyl) amide			
	$[eFAP]^-$	tris(pentafluoroethyl)trifluorophosphate			

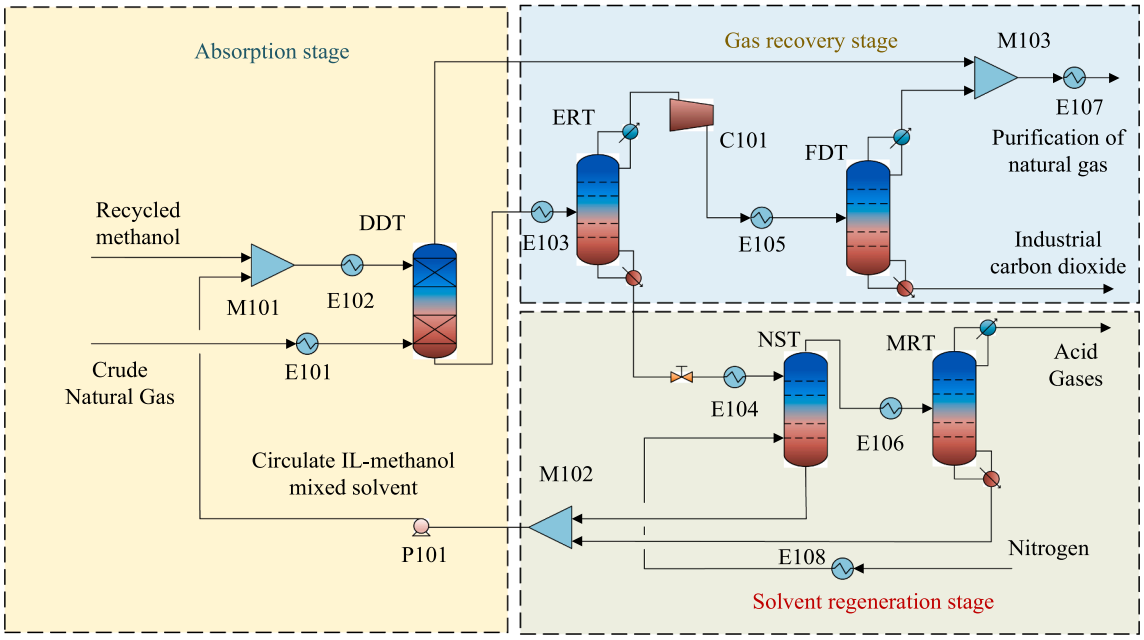

Fig. 3. Natural gas upgrading process using IL-methanol mixed solvent.

utilized. Furthermore, the minimum and maximum numbers of substituents n_S^L, n_{Sl}^L and n_S^U, n_{Sl}^U are, respectively, specified for the cation and each side chain l, considering the size and complexity of the designed IL candidates, as shown in (Eqs. (6) and (7)).

The IL pure property constraints of viscosity (η) and melting point (T_m) are, respectively, expressed by Eqs. (8) and (9), where k represents the total number of different groups in the molecule, n_i denotes the number of groups of type i and the group contributions are described as $a_{i,\eta}$, $b_{i,\eta}$, $d_{i,\eta}$, and Δt_i [59,60]. Eq. (10) is used to fulfill the necessary and sufficient conditions for the phase stability of the IL-methanol mixture. In this equation, x_{IL} denotes the mole fraction of IL in this binary mixture and the activity coefficient of IL, γ_{IL}, can be calculated from UNIFAC-IL model. Meanwhile, the removal selectivity of H_2S/CH_4 (β_{H_2S,CH_4}) and CO_2/CH_4 (β_{CO_2,CH_4}) are described by Eqs. (11) and (12), where $P_{CH_4}^S$, $P_{H_2S}^S$,$P_{CO_2}^S$ are the vapor pressure and $\gamma_{CH_4}^\infty$, $\gamma_{H_2S}^\infty$, $\gamma_{CO_2}^\infty$ are the infinite dilute activity coefficient of CH_4, H_2S and CO_2, respectively. Eq. (13) gives a process model constraint describing the composition of a binary mixture in terms of the mole fraction of IL and methanol ($x_{methanol}$).

2.2. Solvent targeted removal of acid gases

While searching for a mixed solvent is selective toward removing CO_2, the objective function of the design problem can be described as following:

$$max_{z,y} f(z,y) = \frac{\gamma_{CH_4}^\infty \gamma_{MeOH,CH_4}^\infty}{M_{IL}\gamma_{CO_2}^\infty \gamma_{MeOH,CO_2}^\infty} \tag{14}$$

In contrast, when searching for a mixed solvent is selective toward

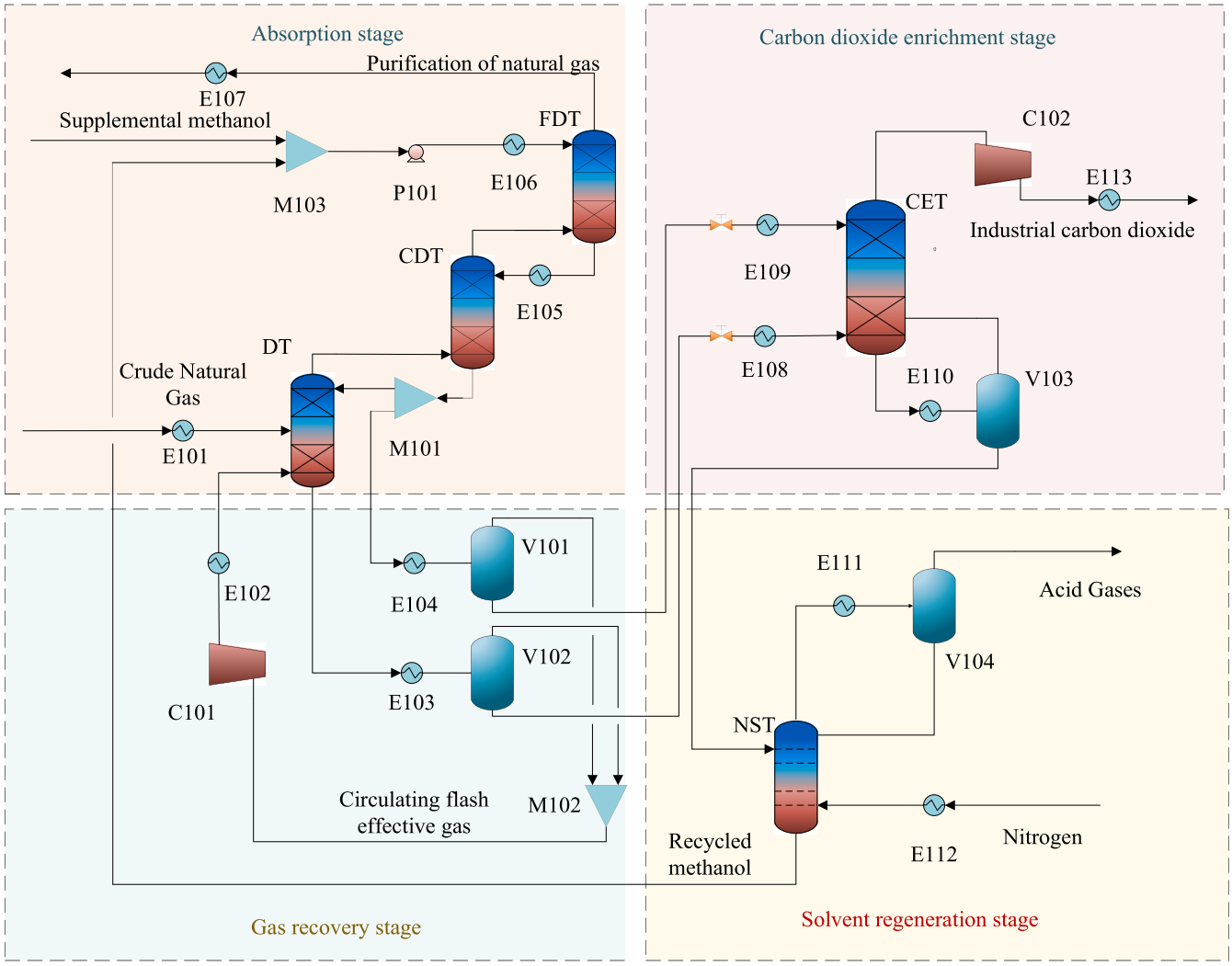

Fig. 4. Rectisol process.

Table 3
Composition and status of raw natural gas.

Component (Mole fraction, %)	Value
CH_4	77.53
C_2H_6	0.01
C_3H_8	0.00
H_2S	14.90
CO_2	7.14
H_2	0.01
N_2	0.41
Temperature (℃)	25
Pressure (bar)	80
Mole flow (kmol/h)	10,800
Mass flow (kg/h)	224386.37

removing H_2S, the objective function of the design problem can be described as follows:

$$max_{z,y} f(z,y) = \frac{\gamma^{\infty}_{CH_4}\gamma^{\infty}_{MeOH,CH_4}}{M_{IL}\gamma^{\infty}_{H_2S}\gamma^{\infty}_{MeOH,H_2S}} \tag{15}$$

In Eqs. (14) and (15), $\gamma^{\infty}_{MeOH,CH_4}$ $\gamma^{\infty}_{MeOH,CO_2}$ and $\gamma^{\infty}_{MeOH,H_2S}$ are the infinite dilute activity coefficient of CH_4, CO_2 and H_2S in methanol, respectively. The molar weight (M_{IL}) of different ILs varies a lot but their cost is mostly based on the weight consumption. For this reason, M_{IL} is also included in the objective function.

3. Result

In this section, a case study on the natural gas upgrading process is carried out to investigate the potential of using an IL-methanol mixed solvent. One of the world's largest natural gas purification plants in China is taken as the case. The annual processing capacity of raw natural gas (high-sulfur) in this plant is 12 billion cubic meters. The purification standards for the two main acid gases are H_2S content $\leq$6 mg/m^3 and

Table 4
Required information on IL for the process simulation in Aspen Plus.

Solvents	MW (g/mol)	API gravity	T_{nb} (K)	Tc (K)	*Pc* (MPa)	Vc (m^3/kmol)	η (mPa s, 273 K)	ω
[C_1OHPy] [TFA]	224	36.5	457	553	0.77	0.96	4.91	0.77

Table 5
Operating parameters for simulating the natural gas upgrading process in Aspen Plus.

Operating Unit	Simulation model	Description of operating conditions
Natural gas upgrading process using IL-methanol mixed solvent.		
DDT	RadFrac (Absorber)	Number of stages:15; Pressure: 80 bar; Feed temperature: 25 ℃ (S1) and 25 ℃ (S4)
MRT	RadFrac	Number of stages: 45; Pressure: 40 bar; Feed location: 25; Reflux ratio (mol): 1; Feed temperature: S6 (60 ℃)
FDT	RadFrac	Number of stages: 60; Pressure: 45 bar; Feed location: 30; Reflux ratio (mol): 7; Feed temperature: S13 (−20 ℃)
SDT	RadFrac (Absorber)	Number of stages: 30; Pressure: 1 bar; Feed temperature: S27 (25 ℃) and S11 (52 ℃)
MRT	RadFrac	Number of stages: 30; Pressure: 0.3 bar; Feed location: 15; Reflux ratio (mol): 0.4; Feed temperature:50 ℃
Rectisol process		
DT	RadFrac (Absorber)	Number of stages: 60; Pressure: 45.5 bar; Feed temperature: S2 (−30 ℃), S40 (−30 ℃), S4 (−1 ℃)
CDT	RadFrac (Absorber)	Number of stages: 8; Pressure: 45.4 bar; Feed temperature: S3 (3 ℃), S8 (−30 ℃)
FDT	RadFrac (Absorber)	Number of stages: 14; Pressure: 44.4 bar; Feed temperature: S11 (−50 ℃), S5 (−15 ℃)
CET	RadFrac (Absorber)	Number of stages: 45; Pressure: 2.5 bar; Feed temperature:S18 (−60 ℃), S26 (−40 ℃), S31 (22 ℃)
NST	RadFrac (Absorber)	Number of stages: 30; Pressure: 0.5 bar; Feed temperature: S32 (22 ℃), S34 (0 ℃), S37 (80 ℃)
V101	Flash	Pressure: 5 bar; Temperature:44 ℃
V102	Flash	Pressure: 5 bar; Temperature: −8 ℃
V103	Flash	Pressure: 2.5 bar; Temperature:22 ℃
V104	Flash	Pressure: 5 bar; Temperature: 0 ℃

$CO_2 \leq 3$ mass%.

Due to the raw natural gas having a very high H_2S content, we apply the MINLP problem to identify the mixed solvent preparation in this case, targeting the highest affinity towards H_2S, while keeping the affinity to CO_2 as a design constraint. Conversely, when the raw natural gas contains more CO_2 and less H_2S, we preferentially target the affinity to CO_2. Indeed, it would also be possible to consider both components in a multi-objective function. However, due to the presence of a large number of integer and binary variables in the formulated MINLP problem, combining an objective function with a design constraint would result in much better computational performance than its multi-objective counterpart.

In this work, the identification of the optimal IL is obtained through solving a formulated computer-aided ionic liquid design (CAILD)-based MINLP problem. A total of 1,987,045 structurally feasible IL candidates are generated from a comprehensive combination of 20 cation groups, 17 anion groups, and 5 substitute groups (Eqs. (1)–(7)), and out of these, 608,405 meet the given temperature constraint (Eq. (9)). After imposing the viscosity constraint (Eq. (8)), 48,720 IL candidates remain. After combining all other design constraints (Eqs. (11) and (12)), 1-methyl-3-hydroxyl-pyridinium trifluoroacetate ([C_1OHPy][TFA]) with the highest separation performance towards H_2S, as defined by Eq. (15), is selected for further evaluation. The phase stability of the IL-methanol mixture is constrained by Eq. (10), and a process model constraint is expressed by Eq. (13). Table 2 presents the detailed information for the building blocks of the IL in this CAILD-based MINLP problem.

The hydroxy group is a common functional group found in many ionic liquids. It can significantly influence the properties and behavior of the IL, especially when attached to the aromatic ring of the cation. The influences associated with the studied process can be summarized as follows: (1) The presence of the hydroxy group can enhance the polarity and solubility of the IL in polar solvents (such as methanol). The hydroxy group can form hydrogen bonds with other molecules, increasing the interactions between the IL and its surroundings. (2) The hydroxy group can also contribute to higher viscosity in the IL due to increased molecular interactions. (3) The presence of hydroxy groups can influence the melting and boiling points of the IL. On the other hand, the position of the hydroxy group on the aromatic ring is also important, as it can affect the steric hindrance, hydrogen bonding potential, and electronic interactions of the IL. The hydrogen bonding strength between hydroxyl groups and the nitrogen atom in pyridine varies at different substitution

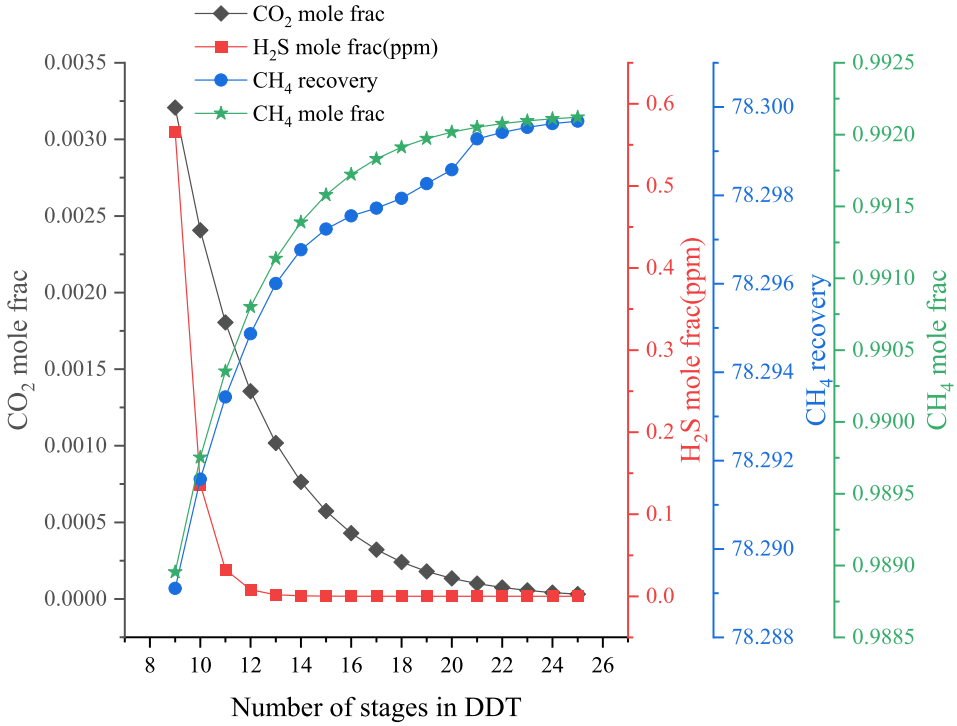

Fig. 5. Influence of theoretical plate number on absorption effect.

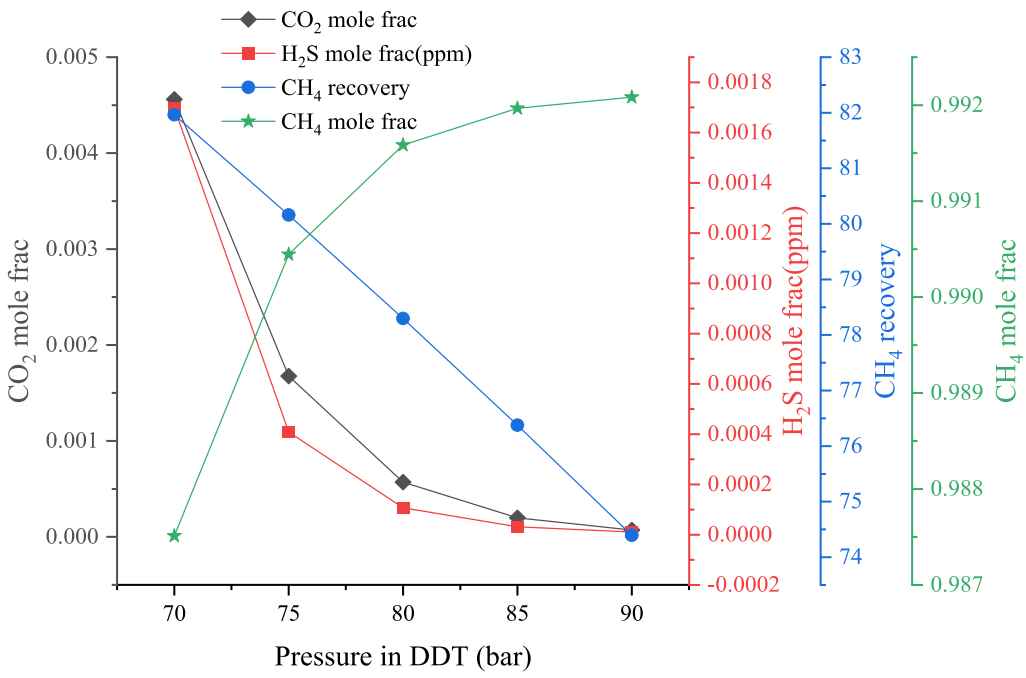

(a)

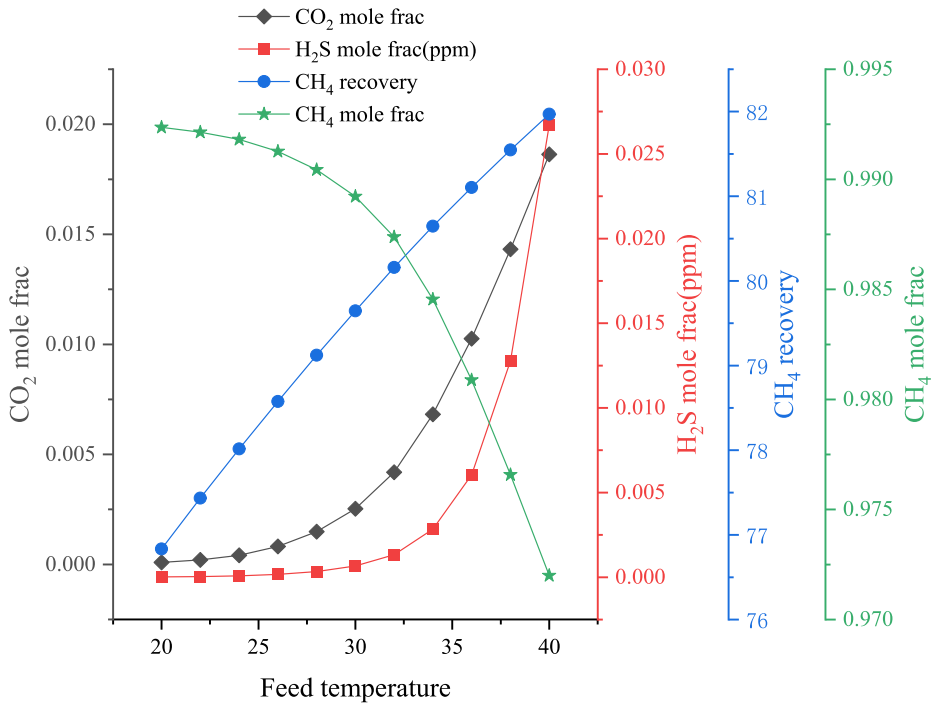

(b)

Fig. 6. Effects of absorption pressure (a), ionic liquid-methanol mixture feed temperature (b), and an ionic liquid mass fraction (c) on methane recovery and natural gas purity.

positions, resulting in different entropy effects. Due to the influence of the nitrogen atom on the pyridine ring, the electron cloud density at the ortho and para positions is lower than that of the benzene ring. As a result, the substituent groups mainly enter the meta (β) position. Therefore, the preparation of 3-hydroxypyridine-based ILs is relatively simple and cost-effective [61].

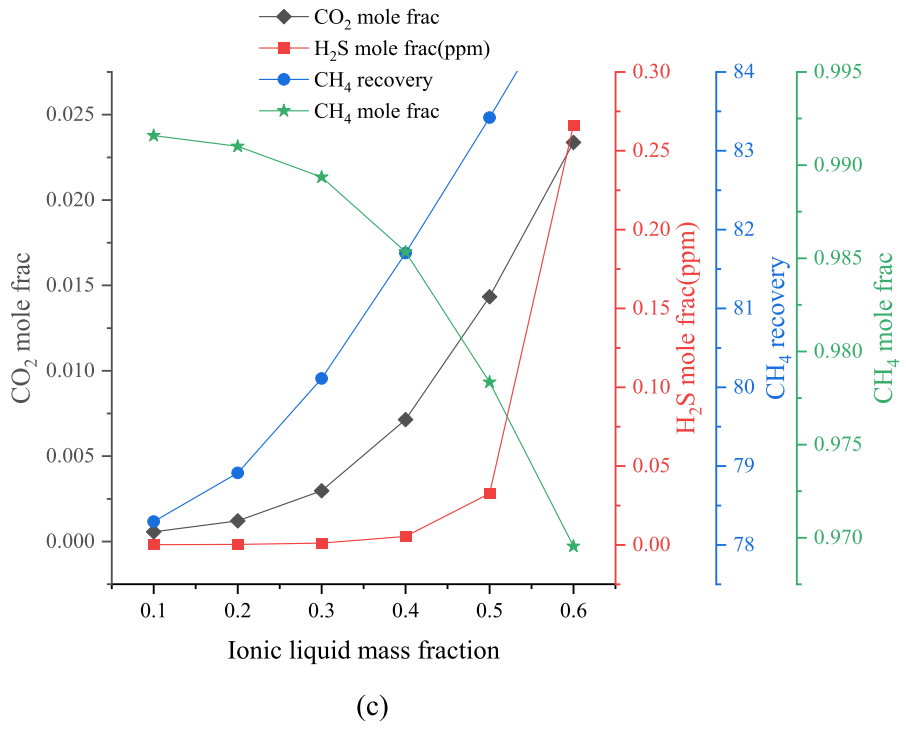

Fig. 6. (*continued*).

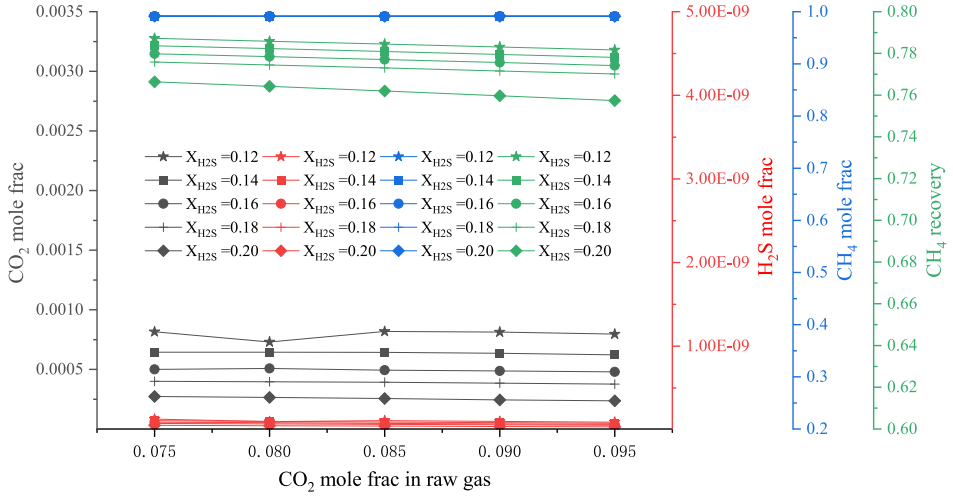

Fig. 7. Influence of H_2S and CO_2 concentrations in raw natural gas on the recovery of CH_4 and the purity of sweet gas.

3.1. *Process Description and simulation*

3.1.1. *Natural gas upgrading process of IL-methanol mixed solvent*

A natural gas upgrading process utilizing IL-methanol mixed solvent is proposed in this paper. The process is divided into three main stages: absorption of acidic gas components (H_2S/CO_2) in natural gas, recovery of entrained CH_4, and recovery of IL-methanol mixed solvent. In the H_2S/CO_2 absorption section, the acid gas components are absorbed by a single tower at high pressure and room temperature (80 bar, 25 ℃). In the recovery section, where entrained CH_4 is recovered, and in the regeneration section of IL-methanol mixed solvent, the stronger adsorption of H2S in the IL-methanol mixed solvent allows for the desorption of entrained CH_4 and CO_2. Since CH_4 and CO_2 have different relative volatilities, they can be separated using a distillation column. The remaining H_2S in the IL-methanol mixture is removed using an N_2 stripper, and the IL-methanol mixture is then recovered. The flowsheet of the proposed natural gas upgrading process using IL-methanol mixed solvent comprises three stages: (1) acid gas absorption process, (2) gas recovery stage, and (3) solvent regeneration stage, as shown in Fig. 3. Crude natural gas is sent to the bottom of the desulfurization and decarbonization tower (DDT), while the makeup IL-methanol mixed solvent, along with the recycled one, is fed at the top of the DDT to absorb H_2S and CO_2. Industrial-grade methane is obtained at the top of this tower, while the rich liquid containing acidic gas is sent to the methane recovery tower (ERT), where most of the absorbed CH_4 and CO_2 are recovered at an optimized reflux ratio and pressure. The mixture of CH_4 and CO_2 is compressed and then sent to the fine decarbonizing tower (FDT) for further refining. The CH_4 separated from the top of the FDT, combined with the CH_4 from the top of the DDT, accounts for industrial-grade natural gas with a molar purity of 99.2. Meanwhile, an industrial-grade CO_2 product is also collected from the bottom of the FDT. On the other hand, a nitrogen stripping tower (NST) is employed to

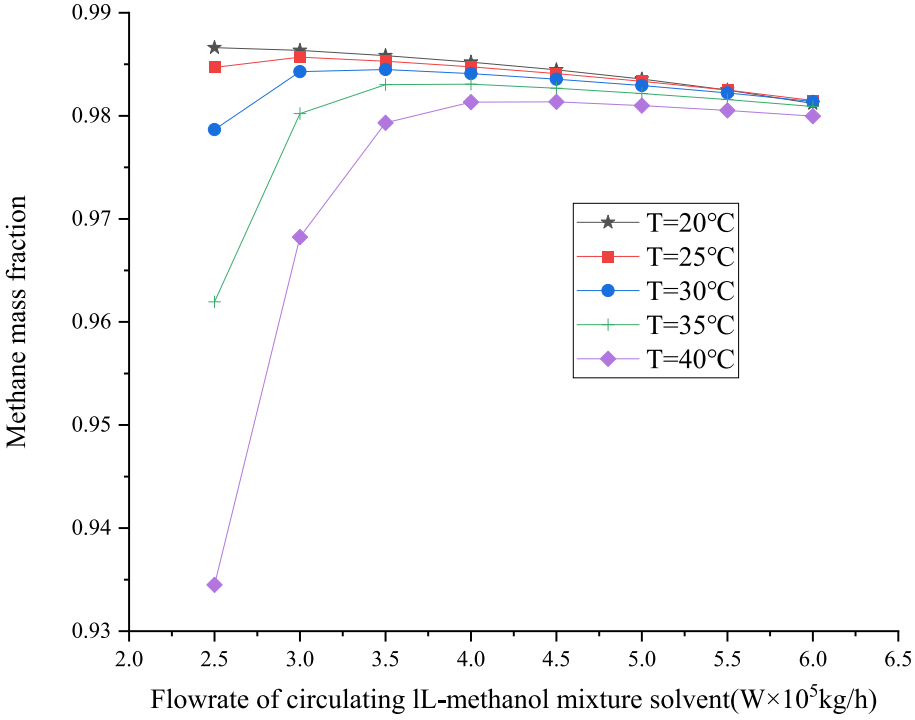

Fig. 8. Influence of pressure (a) and reflux ratio (b) in the distillation column on the recovery of CH_4 and the purity of sweet gas.

Table 6
Key operating parameters of the natural gas upgrading process with IL-methanol mixed solvent.

Operation parameter	Number of stages	IL mass fraction	Absorbent feed temperature (℃)	Tower absorption pressure (bar)	Circulating absorbent flow rate (W × 10^5 kg/h)
DDT tower	20	0.1–0.2	25	80	2.5–3

process the semi-lean liquid containing H_2S that comes from the bottom of the ERT. Meanwhile, a methanol recovery tower (MRT) is applied to avoid solvent loss and recover the methanol emitted from the top of the ERT. Finally, the regenerated IL-methanol mixed solvent is pumped back to the DDT after mixing with a small amount of makeup solvent. Interestingly, this process can produce both high-quality natural gas and industrial-grade CO_2 simultaneously.

3.1.2. *Rectisol process*

The Rectisol process primarily consists of four parts: absorption of acidic gas components (H_2S/CO_2) in natural gas, recovery of entrained CH_4, carbon dioxide enrichment, and methanol solvent regeneration. The absorption section for H_2S/CO_2 utilizes three absorption towers in series to gradually absorb H_2S and CO_2. The recovery of CH_4 is achieved through flash evaporation of the methanol-rich liquid by increasing the temperature and reducing the pressure. Most of the CH_4 evaporates and is returned to the absorption tower via a compressor. In the carbon dioxide enrichment and methanol solvent regeneration section, CO_2 and H_2S are desorbed step by step, allowing for the regeneration of the methanol solvent and obtaining industrial-grade CO_2 products with a purity of 99 %. The flowsheet of the Rectisol process contains four stages: (1) acid gas absorption process, (2) gas recovery stage, (3) carbon dioxide enrichment stage, and (4) solvent regeneration stage, as shown in Fig. 4. Firstly, crude natural gas is sequentially processed in the desulfurization tower (DT), crude decarbonization tower (CDT), and fine decarbonization tower (FDT) under low temperature (−30 ℃) using methanol as the absorbent. Natural gas product with a molar purity of 99.3 % is obtained at the top of the FDT, while the acid gas-rich liquid (also containing a certain amount of CH_4) is sent to the gas recovery stage. In the gas recovery stage, the absorbed CH_4 is recovered by reducing the pressure and temperature in flash tanks V101 and V102. The recovered CH_4 is then sent back to the bottom of the DT after being compressed at C101. Meanwhile, the residual liquid from V101 and V102 is sent to a carbon dioxide enrichment tower (CET), where an industrial-grade CO_2 product with a purity of 99 % is obtained at the top of the tower. On the other hand, the liquid at the bottom of the CET is sent to flash tank V103, where the remaining CO_2 is desorbed and sent back to the CET, and the semi-lean liquid containing most H_2S is sent to a nitrogen stripping tower (NST). The methanol regenerated at NST is recycled to the FDT after mixing with a small amount of supplemental solvent. Additionally, a methanol recovery flash tank, located beside the stripping tower, is used to recover the methanol carried by the acidic gas, facilitating further treatment of the acidic gas.

3.2. *Process modeling and simulation*

Process simulation involves creating a model-based representation of chemical and other technological processes in software, providing valuable insights into the process before its actual industrial implementation. In this section, Aspen Plus, a commercial software, was used to simulate the natural gas upgrading process through both IL-methanol mixed solvent-based and Rectisol technologies. The goal was to optimize the process parameters for the studied natural gas upgrading processes. The specific process simulation diagram is shown in Fig. S1. Aspen Plus does not include ILs in its component database, so they are typically introduced as pseudo-components by specifying their molecular information, such as molar mass, psychological properties, and critical properties. In this case, the physical properties of the ILs were calculated using the group contribution method proposed in our previous work [62], and their critical properties were estimated using the fragment contribution-corresponding state method proposed by Huang et al. and Ying Huang [63] et al. (as shown in Table 4). Additionally, a suitable thermodynamic model is required to predict the thermodynamic

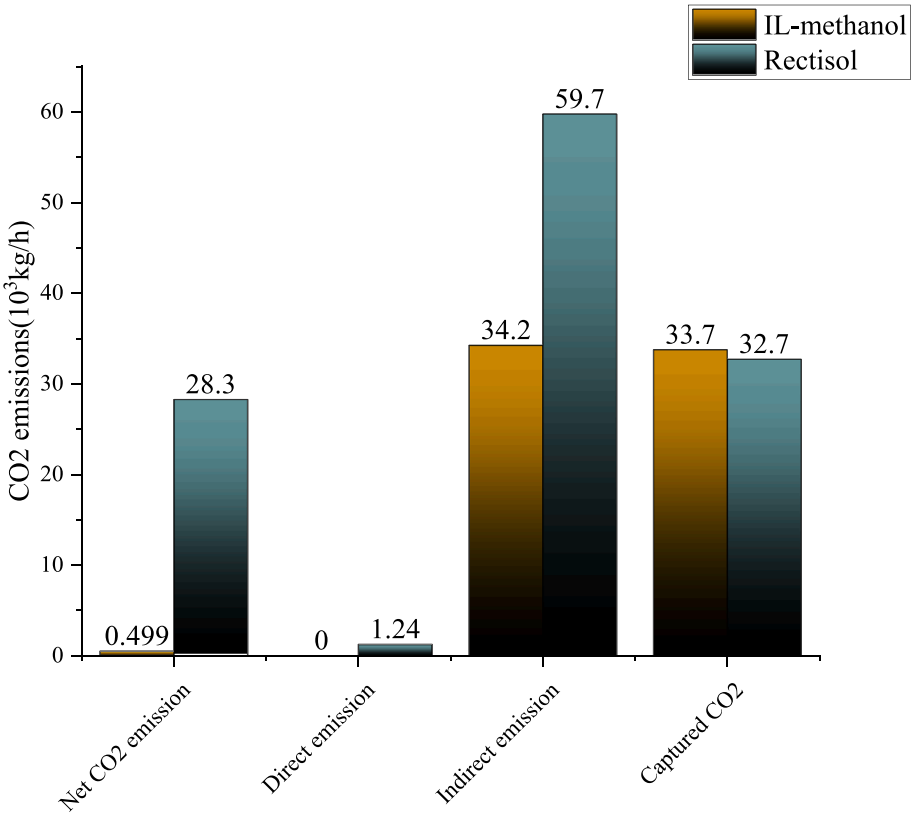

Fig. 9. Carbon dioxide emission analysis was performed for the two processes.

behavior of the IL-containing system under study. The UNIFAC model, which has been applied in previous studies was used in the simulation [64,65]. Furthermore, in the simulation, various unit operations are involved in these two processes, including absorption, distillation, and fluid flow. The equation of state method and activity coefficient method is commonly used to calculate physical parameters. The NRTL method is employed for the natural gas upgrading process using IL-methanol mixed solvent, while the PSRK method is used for the Rectisol process [24]. Model parameters, such as van der Waals parameters and group interaction parameters of ILs, are directly derived from the UNIFAC-IL gas model proposed in recent work. The gas composition data was taken from Table 3, and the flow rate was obtained directly from the gas company (224,386 kg/h). The specific Aspen simulation process parameters are listed in Table 5.

4. Discussion

To maximize the performance of the proposed natural gas upgrading process, a key parameter analysis of the natural gas upgrading process using IL-methanol mixed solvent is conducted. These optimal operating parameters include the theoretical plate number, the absorption temperature, feed temperature, absorbent flowrate, *etc*.

4.1. Key parameters analysis

4.1.1. Determination of theoretical plate number of absorber

Regarding the natural gas upgrading process using IL-methanol mixed solvent, a high-pressure and normal temperature single tower absorption method is employed. The absorption efficiency of the Desulfurization and Decarbonization Tower (DDT) in the desulfurizing and decarbonizing process not only determines the purity of the natural gas products and the amount of absorbent but also affects the difficulty of absorbent recovery, which has a significant impact on energy consumption and the overall process economy. Therefore, it is crucial to perform parameter analysis of the DDT tower for desulfurization and decarbonization. The following parameters should be considered for assessing the absorption efficiency of the DDT tower: the theoretical number of tower stages, tower collection pressure, temperature and flow rate of the circulating absorber feed, and the proportion of ionic liquid in the absorber to the IL-methanol mixed solvent.

The solvent flow rate and temperature of the IL-methanol mixture were initially determined, while keeping the molar flow rate and composition of the raw natural gas unchanged. By varying the number of theoretical stages in the absorber, the absorption efficiency's sensitivity to the number of theoretical stages was analyzed (as shown in Fig. 5). From the figure, it can be observed that as the number of theoretical stages in the absorption tower increases from 9 to 20, the concentration of acid gases, CO_2, and H_2S, significantly decreases. After reaching around 20 theoretical stages, the curves for the concentration of CH_4 and acid gases tend to flatten, and further increases in the number of theoretical stages result in a slower decline in the concentration of acid gases. The number of theoretical stages has an impact on the equipment cost of the tower, while the amount of absorbent affects the cost of subsequent absorbent regeneration. Therefore, achieving a separation task with low total operating and equipment costs is feasible when employing approximately 20 theoretical stages.

4.1.2. Influence of the temperature and composition of the absorber and the absorption pressure of the tower on the absorption effect

By utilizing the control variable method, the effects of varying the absorption pressure, the feed temperature of the ionic liquid-methanol mixture, and the mass fraction of the IL on methane recovery, acid gas absorption efficiency, and natural gas purity were investigated (as shown in Fig. 6). When solely adjusting the absorption pressure, it is observed that increasing the absorber pressure results in higher molar purity of natural gas in the product and lower concentrations of impurity

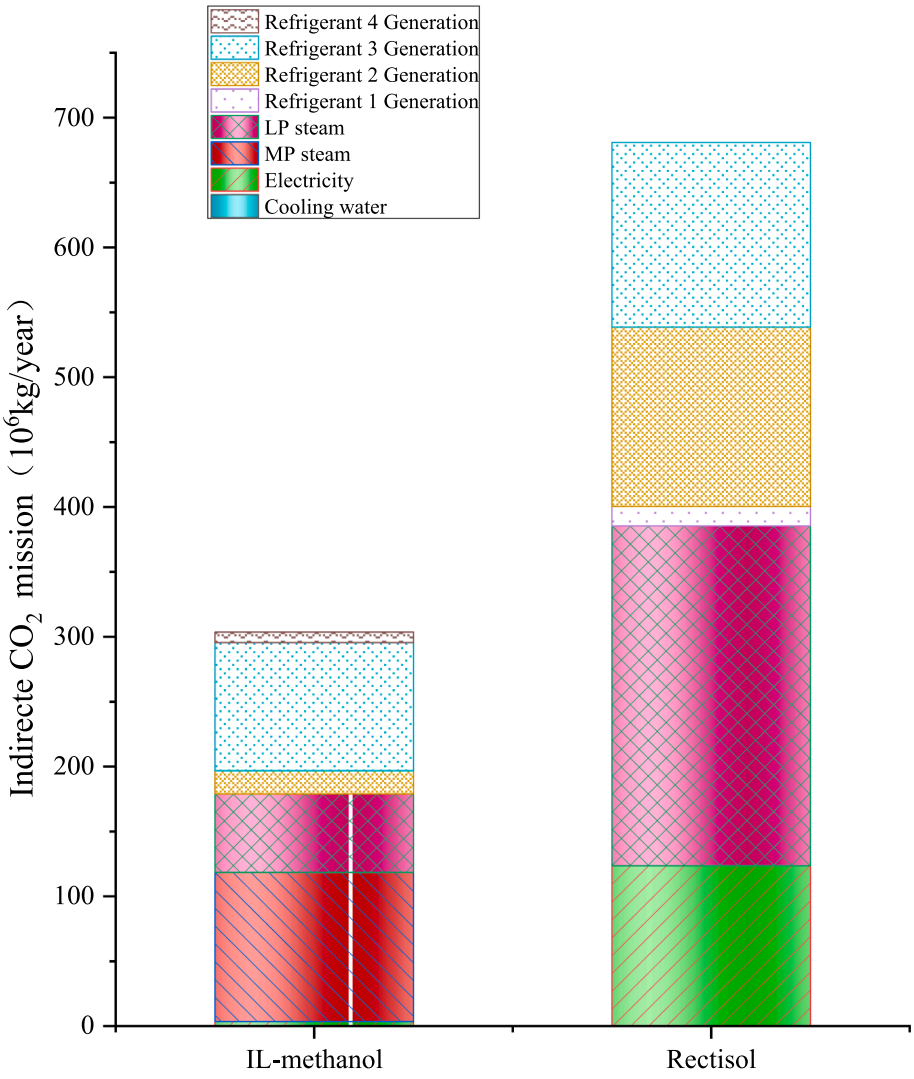

Fig. 10. Indirect carbon dioxide emission analysis was carried out for the two processes.

acid gases, H_2S, and CO_2 (Fig. 6a). In other words, higher pressure enhances the absorption efficiency of acid gases while decreasing the recovery rate of CH_4 in the absorber. As the absorption pressure increases from 70 bar to 80 bar, the molar fraction of CH_4 rises from 98.75 % to 99.16 %, the molar fraction of H_2S decreases from 0.17 %ppm to 0.01 % ppm, and the molar fraction of CO_2 decreases from 0.46 % to 0.05 %. However, when the absorption pressure exceeds 80 bar, the mole fraction curves of CH_4 and acid gases in the product plateau, indicating a diminishing absorption efficiency with further pressure increase. Moreover, the recovery rate of CH_4 exhibits a nearly linear decline with increasing absorption pressure, resulting in higher subsequent treatment costs for the CH_4 recovery section. Therefore, a balance between molar purity and CH_4 recovery rate needs to be considered. Specifically, at 80 bar, the molar content of CO_2 can be controlled to be less than 3 %, ensuring the completion of the absorption task at a lower cost while meeting the quality requirements for Class I natural gas in the industrial standard.

On the other hand, when only the temperature of the IL-methanol mixed solvent is modified, it is observed that increasing the feed temperature leads to lower molar purity of natural gas in the product and higher concentrations of impurity acid gases, H_2S, and CO_2 (Fig. 6b). In other words, the absorption efficiency of acid gases deteriorates with rising feed temperature, while the recovery rate of CH_4 in the absorber improves. As the feed temperature surpasses 25 ℃, the molar purity of CH_4 in the product gas experiences a significant decrease, accompanied by a notable increase in the molar purity of H_2S and CO_2. Notably, the absorption efficiency of CO_2 is more sensitive to changes in feed temperature. When the feed temperature increases from 20–25 ℃, the molar fraction curve of CH_4 and acid gases in the product exhibits a relatively gradual trend. At this point, the impact of feed temperature variations on the composition and purity of the product is minimal. Taking into account the recovery rate of CH_4, the temperature of the ionic liquid-methanol mixed solvent should be maintained at 25 ℃. Furthermore, when solely altering the mass fraction of the ionic liquid in the ionic liquid-methanol mixed solvent, it is observed that increasing the mass fraction of the ionic liquid leads to lower molar purity of natural gas in the product and higher concentrations of impurity acid gases, H_2S, and CO_2 (Fig. 6c). In other words, a higher mass fraction of the ionic liquid in the mixed solvent results in a poorer absorption effect for acid gases. This implies that the absorption efficiency of the ionic liquid is not as effective as that of methanol. However, the advantage of incorporating the ionic liquid lies in its ability to operate at room temperature and significantly reduce the cooling load. The change in the CO_2 curve is more pronounced compared to that of the H_2S curve, indicating that the absorption effect of CO_2 is more sensitive to variations in the mass fraction of the ionic liquid in the IL-methanol mixed solvent. It is recommended to maintain a mass fraction of 0.1–0.2 for the ionic liquid in the mixed solvent of ionic liquid and methanol.

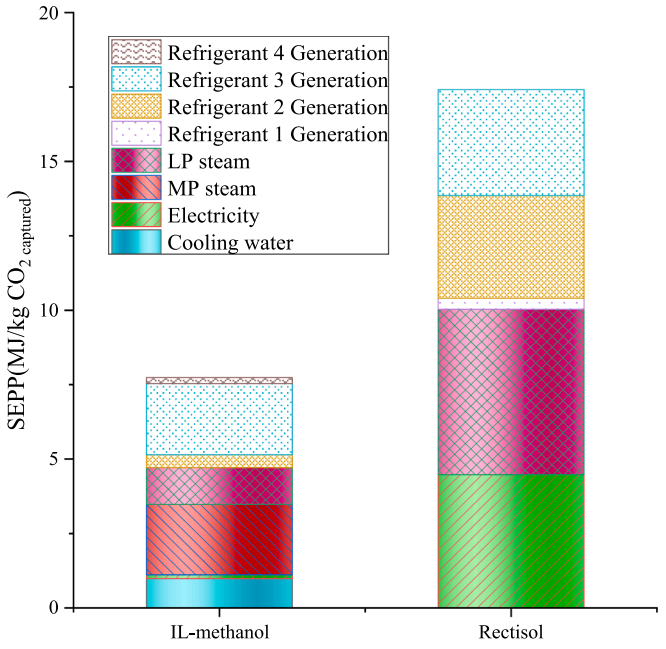

Fig. 11. Comparison of energy consumption of natural gas upgrading process with Rectisol washing and IL-methanol mixed solvent.

4.1.3. H_2S/CO_2 selectivity performance of the IL-methanol mixed solvent

The composition range of natural gas can vary significantly based on the type, depth, and location of underground reservoirs, and it may even change over time, posing challenges to the purification process. Fig. 7 illustrates that while keeping the amount of absorbent and the total molar flow rate of raw natural gas constant, along with the unchanged operating conditions of the absorption tower, the molar ratios of CO_2 and H_2S in the raw natural gas were adjusted. The purified CH_4 molar ratios were all above 99.1 % and met the purification standards for the two main acidic gases (H_2S content $\leq$6 mg/m^3 and $CO_2 \leq$ 3 mass%, respectively). This indicates that the H_2S/CO_2 selectivity of the IL methanol mixed solvent for natural gas, corresponding to different H_2S and CO_2 concentrations, remains essentially unchanged, allowing it to be applied to a wider range of natural gas compositions.

4.1.4. Influence of temperature and flow rate of circulating absorbent on absorption effect

The impact of circulating absorbent temperature and flow rate on the absorption effect is depicted in Fig. 8. When the flow rate of the circulating ionic liquid-methanol mixture is held constant, the influence of temperature on the absorption effect aligns with Fig. 6b. In other words, as temperature increases, the mass fraction of CH_4 in the natural gas product gradually decreases. Conversely, when the temperature of the circulating absorber remains unchanged, the mass fraction of CH_4 initially increases and then decreases with an increase in the flow rate of the absorber. At flow rates ranging from 250,000 to 300,000 kg/h of the circulating ionic liquid-methanol mixture, the mass fraction of CH_4 in the natural gas product starts to decline as the flow rate of the mixed absorber continues to increase. This situation may arise due to the relatively lower absorbent flow rate. Since the absorbent exhibits higher selectivity towards acid gas, it absorbs acid gas from the raw natural gas more readily than methane, resulting in an increased mass fraction of CH_4 in the product. However, when the absorbent flow rate exceeds 300,000 kg/h, most of the acid gas in the natural gas has already been absorbed, and the primary target for the mixed absorbent becomes CH_4. As a result, the purity of CH_4 in the product decreases. Furthermore, further increasing the quantity of circulating absorbent leads to higher energy consumption and increased investment costs in solvent recovery and regeneration processes. The key operating parameters for the natural gas upgrading process with IL-methanol mixed solvent, determined through process simulation and sensitivity analysis, are presented in Table 6.

4.2. Environmental assessment

Environmental friendliness can be assessed by calculating CO_2 emissions using the following formula [64]:

$$\text{Net}\,CO_2\text{emission} = \text{Directemission} + \text{Indirectemission} - \text{Captured}CO_2 \tag{16}$$

The carbon emission results of the studied natural gas upgrading processes are presented in Fig. 9. As observed, the Rectisol process exhibits a direct CO_2 emission of 1.24 $\times$ 10^3 kg/h, whereas the process using IL-methanol mixed solvent shows no direct carbon emissions. Meanwhile, there are indirect CO_2 emissions from hot and cold utilities. For the natural gas upgrading process using IL-methanol mixed solvent, these emissions were measured at 3.42 $\times$ 10^4 kg/h, whereas for the Rectisol process, they amounted to 5.97 $\times$ 10^4 kg/h. Consequently, the indirect CO_2 emissions for the natural gas upgrading process with IL-methanol mixed solvent were 42.71 % lower compared to those of the Rectisol process. Ultimately, the net emission of the natural gas upgrading process with IL-methanol mixed solvent was found to be 98.23 % less than that of the Rectisol process, demonstrating significant advantages of our proposed IL-methanol-based natural gas upgrading technology. Indirect carbon dioxide emission analysis was conducted for the two processes, as shown in Fig. 10. The molar concentration of methanol in the purified natural gas is only 0.1 %, and the loss of methanol is 333.23 kg/hr.

4.3. Energy analysis

In this section, Aspen Energy Analyzer V11 is employed to analyze the energy integration of the natural gas upgrade process and the Rectisol process for the IL-methanol mixed solvent. The specific equivalent power penalty (SEPP) is utilized as a crucial parameter to evaluate the overall energy consumption during process evaluation, particularly for energy-intensive processes. The SEPP can be defined as follows [44,66]:

$$SEPP = \frac{\eta\left(Q_{cooling} + Q_{heating}\right) + E_{compression} + E_{fuel}}{m_{CO_2}} \tag{17}$$

Table 7
Clamp force analysis and HEN performance results for the optimal design.

Items	Rectisol			Natural gas upgrading process using IL-methanol mixed solvent		
	Targets	HEN performance	Percent of target (%)	Targets	HEN performance	Percent of target (%)
Heating duty (kJ/h)	4.01 × 10^7	8.45 × 10^7	210.76	2.14 × 10^8	2.21 × 10^8	103.37
Cooling duty (kJ/h)	1.89 × 10^8	2.33 × 10^8	123.53	2.47 × 10^8	2.54 × 10^8	102.92
	Cost index targets	Network indexes	Percent of target (%)	Cost index targets	Network indexes	Percent of target (%)
OPEX ($/year)	6.96 × 10^6	9.56 × 10^6	4.33 × 10^9	1.21 × 10^7	1.28 × 10^7	3.33 × 10^9
Capital cost ($)	4.59 × 10^7	1.69 × 10^7	36.86	7.46 × 10^6	3.29 × 10^6	44.11
TAC ($/year)	1.91 × 10^7	1.40 × 10^7	2.32 × 10^9	1.41E × 10^7	1.37E × 10^7	3.06 × 10^9
Number of heat exchanges	15	35	/	16	16	/

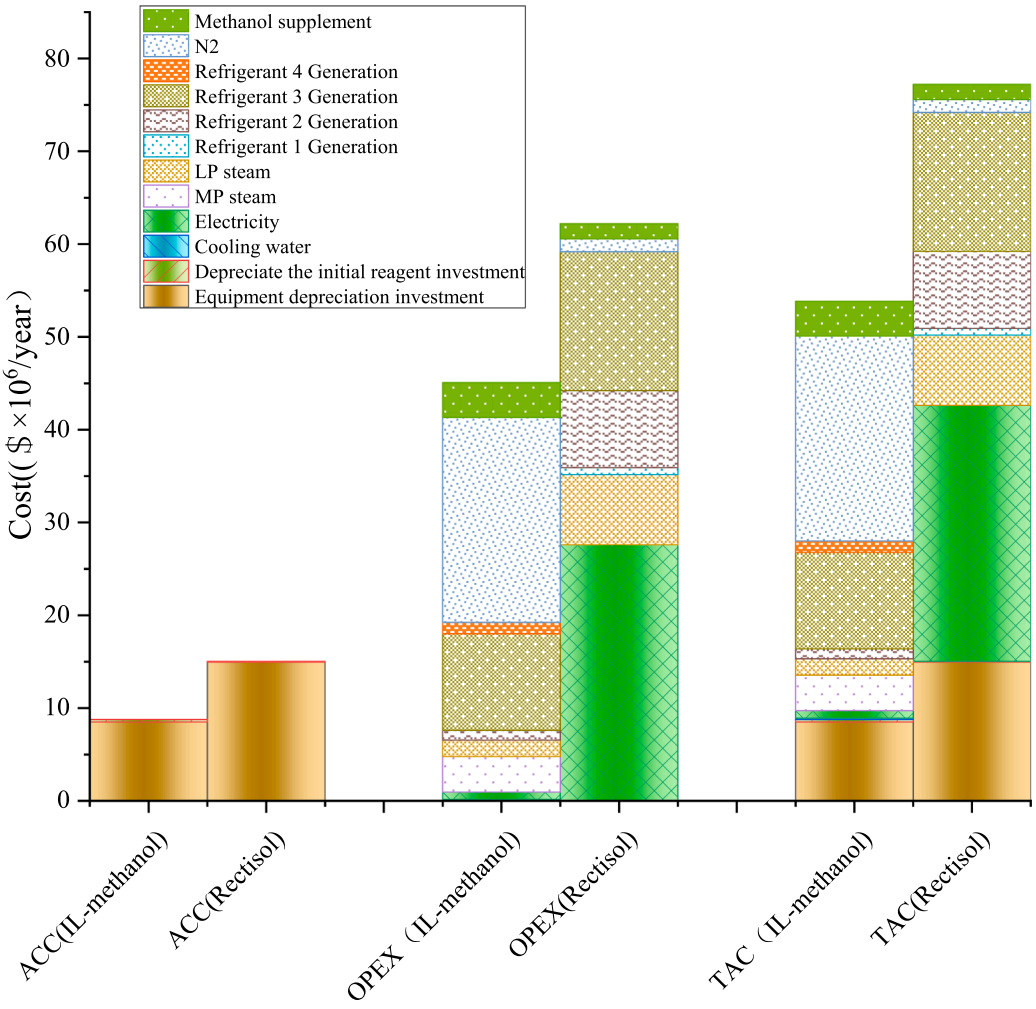

Fig. 12. Total cost (TAC) versus detailed cost in both processes.

Where $Q_{cooling}$ and $Q_{heating}$ represent cooling and heating loads, $E_{compression}$ represents compressed power demand, and E_{fuel} is the chemical exergy of fuel gases captured together with H_2S and CO_2 products. m_{CO_2} is the mass velocity of the captured CO_2 product, η represents the thermoelectric conversion efficiency, which is assumed to be 0.40 [40].

Due to the introduction of ILs into the absorbent, the total energy consumption of the natural gas upgrading process using IL methanol mixed solvent is significantly lower than that of the Rectisol process. The comparison results of the specific equivalent power penalty (SEPP) for the two processes are depicted in Fig. 11. It can be observed that the natural gas upgrading process with IL-methanol mixed solvent requires 7.74 MJ of electricity to capture 1 kg of CO_2, whereas the Rectisol process demands 17.41 MJ of electricity. In comparison to the linear Rectisol process, the natural gas upgrading process with IL-methanol mixed solvent achieves a power saving rate of 55.57 %. The advantages of the natural gas upgrading process with IL-methanol mixed solvent include reducing the total utility load and enabling the absorption of H_2S and CO_2 from natural gas at room temperature.

A heat exchange network (HEN) is an effective energy-saving technology. By improving the inefficient heat exchange, maximizing the utilization of cold and hot logistics for mutual heat exchange, and facilitating heat recovery while minimizing the consumption of heating and cooling public works, the HEN can achieve universal energy efficiency without compromising the logistics process. The heat flow and cold flow data obtained from Aspen Plus V11 are utilized for this purpose. The supply, target temperature, and heat capacity of these logistics are outlined in Table S2. The HEN design is implemented using the heat transfer coefficient and cost coefficient embedded in the Aspen database. In this study, the performance of the generated HEN is evaluated and compared using the annual total cost (TAC). The pinch temperatures for the IL-methanol natural gas upgrading process and the Rectisol process are determined to be 13.1 °C and -37.5 °C, respectively, with a minimum temperature difference (T_{min}) of 2 °C. The overall recombination curve and structure of the optimal HEN for the two processes are illustrated in Figs S2 and S3, respectively. Table 7 presents the HEN performance of the optimized design for the natural gas upgrade process using IL-methanol mixed solvent and Rectisol technologies.

4.4. Economic analysis

In this section, Aspen Economics Analyzer V11 was utilized to analyze the economic benefits of the natural gas upgrading process and the Rectisol process using IL-methanol mixed solvent. The annualized cost of capital (ACC) and the total annualized cost (TAC), which encompasses the total operating costs (OPEX), are commonly employed as economic indicators to evaluate processes. The model parameter information required to calculate the ACC of different devices is provided in Table S1. In the natural gas upgrade process using IL-methanol mixed solvent, although there is no loss of IL in the recovery process, the cost of IL supplementation is not considered. However, the initial investment in IL reagents is included as part of the ACC cost. Both processes involve an N_2 stripping column SDT, and the reagent cost of N_2 is accounted for in the OPEX operating cost. The TAC formula for both processes is as

follows [65]:

$$TAC = ACC + OPEX = \Lambda_i \times \Sigma^c C + \Sigma^c C \quad (18)$$

Where ACC is the equipment investment of methanol and IL recovered ($), OPEX is the operation cost of public works, N_2 reagent cost and fresh methanol replenishing cost ($/y), and Λ_1 is the annualized coefficient of equipment (1/y).

Λ_1 represents the depreciation factor of equipment, and its value can be calculated by the following formula:

$$\Lambda_1 = \frac{\left(1 + \frac{YR}{100}\right)^{PL}}{UL} \quad (19)$$

In this work, the annual run time and utility prices were directly obtained from the database integrated into Aspen Plus. The cost of IL has a direct impact on the TAC of the natural gas upgrading process using an IL-methanol mixture, as shown in Eq. (17). For industrial production considerations, the price of [C_1OHPy][TFA] is assumed to be $50/kg. Compared to the traditional Rectisol process, the ACC was reduced by 41.40 %, the total operating cost (OPEX) was reduced by 19.23 %, and the annual total cost (TAC) was reduced by 23.90 %. Fig. 12 illustrates that OPEX significantly contributes to TAC compared to ACC, emphasizing the importance of parameter optimization in cost reduction.

It is worth mentioning that the cost of IL [C_1OHPy][TFA] is generally higher than many other well-known ILs due to the introduction of the OH group and cation TFA. However, these cost-effective ILs are either not mixable with methanol and/or do not have good separation performance in the natural gas upgrading process. In this work, a total of 1,987,045 structurally feasible IL candidates are generated from a comprehensive combination of 20 cation groups, 17 anion groups, and 5 substituent groups (Table 2). After combining all the design constraints, [C_1OHPy][TFA] with the highest separation performance towards H_2S is identified as the optimal candidate. Moreover, the absorption process operates at high pressure and room temperature, leading to a very limited loss of IL (only 8.88×10^{-5} kg/hr) in the whole natural gas upgrading process. Meanwhile, the cost of the circulating IL is $\$1.25 \times 10^6$, which only accounts for 2.86 % of the annual depreciated capital cost. To evaluate the impact of the IL price on the economic performance of the proposed natural gas upgrading process, we further calculate the marginal price of IL based on the annualized total cost (TAC) of the traditional Rectisol process. The calculation formula is as follow [64]:

$$P_m = \frac{TAC_{\text{Rectisol process}} - \Lambda_1 \times \sum CC_{equipment,IL} \sum OC_{utility,IL}}{(\Lambda_2 \times m_{circulating,IL} + OT \times m_{makeup,IL})} \quad (20)$$

Where $TAC_{\text{Rectisol process}}$ is TAC ($/y), $CC_{\text{equipment, IL}}$ is the capital cost ($) of the natural gas upgrading process with IL-methanol mixed solvent. $OC_{\text{utility, IL}}$ is the operating cost of the natural gas upgrade process with a mixture of L-methanol ($/y). $m_{\text{circulating, IL}}$ is the flow of circulating IL (kg/h). $m_{\text{makeup, IL}}$ is the flow of fresh IL, kg/h. OT is operation time (h/y), Λ_1 is the annualized factor of the device (1/y), Λ_2 is the annualized factor of IL (1/y).

An IL-involed process becomes profitable when the production cost is lower than the marginal price of the IL used. In this study, the break-even point for the natural gas upgrade process using IL-methanol mixed solvent is determined to be $3,410/kg for [$C_1$OHPy][TFA] price. The desired production price of [C_1OHPy][TFA] has been identified to guide the experimental and pilot-scale studies. Furthermore, the results demonstrate that the natural gas upgrading process using the IL-methanol mixed solvent could achieve a 55.57 % power savings and reduce the TAC by 23.90 % compared to the currently used Rectisol process in the industry. These findings highlight the significant potential of the proposed IL-methanol mixed solvent for natural gas production. For future work, it is recommended to conduct IL synthesis ([C_1OHPy][TFA]) along with relevant experimental tests to obtain a reference for production prices.

5. Conclusion

This work proposes a natural gas upgrading process using IL-methanol mixed solvent for desulfurization and decarbonization in natural gas, aiming to achieve lower energy consumption. In this process, [C_1OHPy][TFA] was identified as the optimal candidate for the structure optimization of mission-specific ionic liquids. The optimization was performed based on a CAILD-based MINLP mathematical model, maximizing the mass-based separation performance design goal while satisfying the requirements for efficient H_2S and CO_2 absorption simultaneously. The results from rigorous process simulation and comprehensive sensitivity analysis indicate that both the traditional Rectisol process and the natural gas upgrading process with IL-methanol mixed solvent can yield high-purity products, with a CH_4 product molar fraction of 99.1 % and a CO_2 product molar fraction of 99 %. However, environmental assessment results showed that the natural gas upgrading process with IL-methanol mixed solvent had 42.71 % lower indirect CO_2 emissions and 98.23 % lower net emissions compared to the Rectisol process. Meanwhile, process evaluation results demonstrated that the natural gas upgrading process with IL-methanol mixed solvent outperformed its traditional counterpart. Compared to traditional natural gas desulfurization and decarbonization methods, the natural gas upgrading process with IL-methanol mixed solvent achieved a 55.57 % power savings when considering equivalent power penalty as the evaluation index. Additionally, the process resulted in a 19.23 % reduction in operating cost and a 41.40 % reduction in annualized capital cost, leading to an overall 23.90 % reduction in TAC (Total Annualized Cost).

The study highlights the significant contribution of OPEX (Operational Expenditure) to TAC in the natural gas upgrade process using IL-methanol mixed solvent and the Rectisol process, emphasizing the importance of heat integration and maximum heat recovery. Moreover, the marginal price of [C_1OHPy][TFA] ($3,410/kg IL) is much higher than the reference price for mass production ($50/kg IL), indicating the low investment risk and promising industrial application prospects for this separation technology.

In this work, the thermodynamic and physical property models used were established from a large number of experimental data points, and they have also been validated in many experimental studies. However, experimental verification of this specifically tailored mixed solvent is required for its further industrial application. Nonetheless, the process simulation results obtained from Aspen Plus (a commercial software widely used in the scale-up study of many new technologies) coupled with accurate property models are relatively reliable. Future work will focus on the preparation of the [C_1OHPy][TFA]-methanol mixed solvent and subsequent pilot plant experiments.

CRediT authorship contribution statement

Yang Lei: Conceptualization, Investigation, Writing - original draft. **Lei Du:** Investigation, Data curation. **Xinyan Liu:** Formal analysis, Data curation. **Haoshui Yu:** Methodology, Writing - review & editing. **Xiaodong Liang:** Writing - review & editing. **Georgios M. Kontogeorgis:** Writing - review & editing. **Yuqiu Chen:** Conceptualization, Methodology, Writing - original draft, Writing- review & editing, Supervision.

Declaration of Competing Interest

The authors declare that they have no known competing financial interests or personal relationships that could have appeared to influence the work reported in this paper.

Data availability

Data will be made available on request.

Acknowledgments

The authors gratefully acknowledge the financial support from the National Natural Science Foundation of China (22208253, 21706198) and the Hubei Province Undergraduate Training Program for Innovation and Entrepreneurship (S202110488034, S202210488116X).

Appendix A. Supplementary data

Supplementary data to this article can be found online at https://doi.org/10.1016/j.cej.2023.146424.

References

[1] S. Mathur, G. Gosnell, B.K. Sovacool, et al., Industrial decarbonization via natural gas: a critical and systematic review of developments, socio-technical systems and policy options, Energy Res. Soc. Sci. 90 (2022) 102638–102661.
[2] T.P. Adhi, Y.A. Situmorang, H.P. Winoto, et al., H_2S-CO_2 gas separation with ionic liquids on low ratio of H_2S/CO_2, Heliyon 7 (12) (2021), e08611.
[3] Z. Wang, F. Yan, L. Bai, et al., Insight into CO_2/CH_4 separation performance in ionic liquids/polymer membrane from molecular dynamics simulation, J. Mol. Liq. 357 (2022) 119119–119131.
[4] J. Wang, Z. Song, H. Cheng, et al., Multilevel screening of ionic liquid absorbents for simultaneous removal of CO2 and H2S from natural gas, Sep. Purif. Technol. 248 (2020) 117053–117064.
[5] O.R. Rivas, J.M. Prausnitz, Sweetening of sour natural gases by mixed-solvent absorption: solubilities of ethane, carbon dioxide, and hydrogen sulfide in mixtures of physical and chemical solvents, AIChE J. 25 (6) (1979) 975–984.
[6] H. Al-fnaish, L. Lue, Modelling the solubility of H2S and CO2 in ionic liquids using PC-SAFT equation of state, Fluid Phase Equilib. 450 (2017) 30–41.
[7] M. Zhang, W. Zhu, H. Li, et al., One-pot synthesis, characterization and desulfurization of functional mesoporous W-MCM-41 from POM-based ionic liquids, Chem. Eng. J. 243 (2014) 386–393.
[8] P. Aixia, Z. Lisheng, Y. Yanqiu, Application and research of high sulfur content gas desulfurization and decarbonization process on Puguang gas field, Chem. Eng. Oil Gas 41 (1) (2012) 17–23, in Chinese.
[9] X. Sun, L. Zhu, P. Wang, et al., CO2 removal from natural gas by moisture swing adsorption, Chem. Eng. Res. Des. 176 (2021) 162–168.
[10] J. Tang, J. Chen, Q. Guo, et al., Kinetics research on mixed solvents of MDEA and enamine in natural gas decarbonization process, J. Nat. Gas Sci. Eng. 19 (2014) 52–57.
[11] Y.S. Yu, Y. Li, Q. Li, et al., An innovative process for simultaneous removal of CO2 and SO2 from flue gas of a power plant by energy integration, Energ. Conver. Manage. 50 (12) (2009) 2885–2892.
[12] A.I. Akhmetshina, A.N. Petukhov, A.V. Vorotyntsev, et al., Absorption behavior of acid gases in protic ionic liquid/alkanolamine binary mixtures, ACS Sustain. Chem. Eng. 5 (4) (2017) 3429–3437.
[13] B.P. Mandal, S.S. Bandyopadhyay, Simultaneous absorption of carbon dioxide and hydrogen sulfide into aqueous blends of 2-amino-2-methyl-1-propanol and diethanolamine, Chem. Eng. Sci. 60 (22) (2005) 6438–6451.
[14] A. Ellaf, S. Ali Ammar Taqvi, D. Zaeem, et al., Energy, exergy, economic, environment, exergo-environment based assessment of amine-based hybrid solvents for natural gas sweetening, Chemosphere 313 (2023) 137426–137442.
[15] Y.H. Chan, S.S.M. Lock, M.K. Wong, et al., A state-of-the-art review on capture and separation of hazardous hydrogen sulfide (H2S): recent advances, challenges and outlook, Environ. Pollut. 314 (2022) 120219–120239.
[16] P. Dolejš, V. Poštulka, Z. Sedláková, et al., Simultaneous hydrogen sulphide and carbon dioxide removal from biogas by water-swollen reverse osmosis membrane, Sep. Purif. Technol. 131 (2014) 108–116.
[17] A. Morisato, E. Mahley, Hydrogen sulfide permeation and hydrocarbon separation properties in cellulose triacetate hollow fiber membrane for high hydrogen sulfide contained natural gas sweetening applications, J. Membr. Sci. 681 (2023), 121734.
[18] Y. Yildiz, A new approach to hydrogen sulfide removal, J. Chem. Soc. Pak 44 (2022) 17–27.
[19] L. Sun, R. Smith, Rectisol wash process simulation and analysis, J. Clean. Prod. 39 (2013) 321–328.
[20] Y. Li, C. Zhang, Y. Yu, et al., Design and optimization of VOC control process for tail gas in Rectisol unit based on steady state and dynamic simulation, Process Saf. Environ. Prot. 168 (2022) 820–832.
[21] M. Gatti, E. Martelli, F. Marechal, et al., Review, modeling, heat integration, and improved schemes of Rectisol®-based processes for CO2 capture, Appl. Therm. Eng. 70 (2) (2014) 1123–1140.
[22] Y. Wang, X. Liu, A. Kraslawski, et al., A novel process design for CO2 capture and H2S removal from the syngas using ionic liquid, J. Clean. Prod. 213 (2019) 480–490.
[23] S. Yang, L. Zhang, D. Song, Conceptual design, optimization and thermodynamic analysis of a CO_2 capture process based on Rectisol, Energy 244 (2022) 122566–122583.
[24] N. Gao, C. Zhai, W. Sun, et al., Equation oriented method for Rectisol wash modeling and analysis, Chin. J. Chem. Eng. 23 (9) (2015) 1530–1535.
[25] Z. Ren, Z. Zhou, M. Li, et al., Deep desulfurization of fuels using imidazole anion-based ionic liquids, ACS Sustain. Chem. Eng. 7 (2) (2018) 1890–1900.
[26] T. Liu, Z. Dong, W. Zhu, et al., Prediction of the solubility of acid gas hydrogen sulfide in green solvent ionic liquids via quantitative structure–property relationship models based on the molecular structure, ACS Sustain. Chem. Eng. 11 (9) (2023) 3917–3931.
[27] E.M. Broderick, M. Serban, B. Mezza, et al., Scientific approach for a cleaner environment using ionic liquids, ACS Sustain. Chem. Eng. 5 (5) (2017) 3681–3684.
[28] M.B. Haider, R. Kumar, Solubility of CO_2 and CH_4 in sterically hindered amine-based deep eutectic solvents, Sep. Purif. Technol. 248 (2020) 117055–117065.
[29] K. Huang, Y.-T. Wu, X.-B. Hu, Effect of alkalinity on absorption capacity and selectivity of SO2 and H2S over CO2: substituted benzoate-based ionic liquids as the study platform, Chem. Eng. J. 297 (2016) 265–276.
[30] I. Mejía, K. Stanley, R. Canales, et al., On the high-pressure solubilities of carbon dioxide in several ionic liquids, J. Chem. Eng. Data 58 (9) (2013) 2642–2653.
[31] A.H. Jalili, A. Mehdizadeh, M. Shokouhi, et al., Solubility and diffusion of CO2 and H2S in the ionic liquid 1-ethyl-3-methylimidazolium ethylsulfate, J. Chem. Thermodyn. 42 (10) (2010) 1298–1303.
[32] M.A.M. Althuluth, Natural gas sweetening using ionic liquids, Eindhoven University of Technology (2014) 1–163.
[33] W. Ding, W. Zhu, J. Xiong, et al., Novel heterogeneous iron-based redox ionic liquid supported on SBA-15 for deep oxidative desulfurization of fuels, Chem. Eng. J. 266 (2015) 213–221.
[34] M. Taheri, R. Zhu, G. Yu, et al., Ionic liquid screening for CO2 capture and H2S removal from gases: the syngas purification case, Chem. Eng. Sci. 230 (2021) 116199–116210.
[35] J.F. Brennecke, B.E. Gurkan, Ionic liquids for CO2 capture and emission reduction, J. Phys. Chem. Lett. 1 (24) (2010) 3459–3464.
[36] T. Qureshi, M. Khraisheh, F. Almomani, Cost and heat integration analysis for CO2 removal using imidazolium-based ionic liquid-ASPEN PLUS modelling study, Sustainability 15 (4) (2023) 3370–3393.
[37] X. Liu, Y. Huang, Y. Zhao, et al., Ionic liquid design and process simulation for decarbonization of shale gas, Ind. Eng. Chem. Res. 55 (20) (2016) 5931–5944.
[38] X. Zhang, X. Zhang, H. Dong, et al., Carbon capture with ionic liquids: overview and progress, Energ. Environ. Sci. 5 (5) (2012) 6668–6681.
[39] Y. Chen, J. Woodley, G. Kontogeorgis, et al., Integrated ionic liquid and process design involving hybrid separation schemes, Comput. Aided Chem. Eng. Elsevier (2018) 1045–1050.
[40] X. Liu, Y. Chen, S. Zeng, et al., Structure optimization of tailored ionic liquids and process simulation for shale gas separation, AIChE J 66 (2) (2020) 16794–16808.
[41] R.D. Rogers, K.R. Seddon, Ionic liquids-solvents of the future, Science 302 (5646) (2003) 792–793.
[42] W. Jiang, W. Zhu, Y. Chang, et al., Ionic liquid extraction and catalytic oxidative desulfurization of fuels using dialkylpiperidinium tetrachloroferrates catalysts, Chem. Eng. J. 250 (2014) 48–54.
[43] M. Taheri, C. Dai, Z. Lei, CO2 capture by methanol, ionic liquid, and their binary mixtures: experiments, modeling, and process simulation, AIChE J. 64 (6) (2018) 2168–2180.
[44] M. Taheri, S. Huang, Z. Lei, IL-Emitsol: Ionic liquid based [EMIM][Tf2N] solvent process for selective removal of CO2 and H2S from syngas, Ind. Eng. Chem. Res. 58 (23) (2019) 10007–10017.
[45] B. Kazmi, F. Raza, S.A.A. Taqvi, et al., Energy, exergy and economic (3E) evaluation of CO2 capture from natural gas using pyridinium functionalized ionic liquids: a simulation study, J. Nat. Gas Sci. Eng. 90 (2021) 103951–103964.
[46] Y.J. Heintz, L. Sehabiague, B.I. Morsi, et al., Hydrogen sulfide and carbon dioxide removal from dry fuel gas streams using an ionic liquid as a physical solvent, Energy Fuel 23 (10) (2009) 4822–4830.
[47] X. Wang, S. Zeng, J. Wang, et al., Selective separation of hydrogen sulfide with pyridinium-based ionic liquids, Ind. Eng. Chem. Res. 57 (4) (2018) 1284–1293.
[48] M. Shokouhi, M. Adibi, A.H. Jalili, et al., Solubility and diffusion of H2S and CO2 in the ionic liquid 1-(2-hydroxyethyl)-3-methylimidazolium tetrafluoroborate, J. Chem. Eng. Data 55 (4) (2010) 1663–1668.
[49] M. Safavi, C. Ghotbi, V. Taghikhani, et al., Study of the solubility of CO2, H2S and their mixture in the ionic liquid 1-octyl-3-methylimidazolium hexafluorophosphate: experimental and modelling, J. Chem. Thermodyn. 65 (2013) 220–232.
[50] M.B. Shiflett, A.M.S. Niehaus, A. Yokozeki, Separation of CO2 and H2S using room-temperature ionic liquid [bmim][MeSO4], J. Chem. Eng. Data 55 (11) (2010) 4785–4793.
[51] M.B. Shiflett, D.W. Drew, R.A. Cantini, et al., Carbon dioxide capture using ionic liquid 1-Butyl-3-methylimidazolium Acetate, Energy Fuel 24 (10) (2010) 5781–5789.
[52] P.J. Carvalho, J.A.P. Coutinho, The polarity effect upon the methane solubility in ionic liquids: a contribution for the design of ionic liquids for enhanced CO2/CH4 and H2S/CH4 selectivities, Energ. Environ. Sci. 4 (11) (2011) 4614–4619.
[53] Z. Lei, B. Zhang, J. Zhu, et al., Solubility of CO2 in methanol, 1-Octyl-3-methylimidazolium Bis (trifluoromethylsulfonyl) imide, and their mixtures, Chin. J. Chem. Eng. 21 (3) (2013) 310–317.
[54] M. Ebrahiminejadhasanabadi, W.M. Nelson, P. Naidoo, et al., Investigation of mixed MEA-based solvents featuring ionic liquids and NMP for CO_2 capture: experimental measurement of CO_2 solubility and thermophysical properties, J. Chem. Eng. Data 66 (2) (2021) 899–914.
[55] C. Moya, R. Santiago, D. Hospital-Benito, et al., Design of biogas upgrading processes based on ionic liquids, Chem. Eng. J. 428 (2022) 132103–132111.
[56] A.H. Jalili, M. Rahmati-Rostami, C. Ghotbi, et al., Solubility of H_2S in ionic liquids [bmim][PF_6],[bmim][BF_4], and [bmim][Tf_2N], J. Chem. Eng. Data 54 (6) (2009) 1844–1849.

[57] J. Abdi, M. Hadipoor, S.H. Esmaeili-Faraj, et al., A modeling approach for estimating hydrogen sulfide solubility in fifteen different imidazole-based ionic liquids, Sci. Rep. 12 (1) (2022) 4415–4433.
[58] Y. Chen, X. Liu, J.M. Woodley, et al., Gas solubility in ionic liquids: UNIFAC-IL model extension, Ind. Eng. Chem. Res. 59 (38) (2020) 16805–16821.
[59] Y. Chen, G.M. Kontogeorgis, J.M. Woodley, Group contribution based estimation method for properties of ionic liquids, Ind. Eng. Chem. Res. 58 (10) (2019) 4277–4292.
[60] J.A. Lazzús, A group contribution method to predict the melting point of ionic liquids, Fluid Phase Equilib. 313 (2012) 1–6.
[61] X.Y. Luo, F. Ding, W.J. Lin, et al., Efficient and energy-saving CO2 capture through the entropic effect induced by the intermolecular hydrogen bonding in anion-functionalized ionic liquids, J. Phys. Chem. Lett. 5 (2) (2014) 381–386.
[62] Y. Chen, E. Koumaditi, R. Gani, et al., Computer-aided design of ionic liquids for hybrid process schemes, Comput. Chem. Eng. 130 (2019) 106556–106573.
[63] Y. Huang, H. Dong, X. Zhang, et al., A new fragment contribution-corresponding states method for physicochemical properties prediction of ionic liquids, AIChE J 59 (4) (2013) 1348–1359.
[64] Y. Lei, Z. Yu, Z. Wei, et al., Structure optimization of task-specific ionic liquids targeting low-carbon-emission ethylbenzene production, Sep. Purif. Technol. 308 (2023) 122827–122843.
[65] Y. Lei, Z. Yu, Z. Wei, et al., Energy-efficient separation of propylene/propane by introducing a tailor-made ionic liquid solvent, Fuel 326 (2022) 124930–124941.
[66] J. Chen, H.L. Lam, Y. Qian, et al., Combined energy consumption and CO2 capture management: improved acid gas removal process integrated with CO2 liquefaction, Energy 215 (2021) 119032–119048.